Small Animal Imaging in Drug Development

Martin G. Pomper* and Jae Sung Lee

Johns Hopkins University School of Medicine, Department of Radiology, MD, USA

Abstract: Better mechanistic understanding of disease through mapping of the human and mouse genomes enables rethinking of human infirmity. In the case of cancer, *e.g*., we may begin to associate disease states with their underlying genetic defects rather than with the organ system involved. That will enable more selective, nontoxic therapies in patients who are genetically predisposed to respond to them. Because one of the major goals of molecular imaging research is to interrogate gene expression noninvasively, it can impact greatly on that process. Most of molecular imaging research is undertaken in small animals, which provide a conduit between *in vitro* studies and human clinical imaging. We are fortunate to be able to manipulate small animals genetically, and to have increasingly better models of human disease. The ability to study those animals noninvasively and quantitatively with new, high-resolution imaging devices provides the most relevant milieu in which to find and examine new therapies.

Key Words: Molecular imaging; small animal imaging; drug development; gene expression imaging; PET.

INTRODUCTION

The human and mouse genomes are highly homologous [1]. Knowledge of the complete gene sequence of another mammal will enable the construction of relevant animal models of human disease at an unprecedented rate and with high specificity. We can study those models in a variety of ways, most incorporating invasive techniques destructive to the tissue, or we can image them. With imaging we can perform longitudinal studies on single animals without the sampling error inherent to biopsy; however, the most important attribute of imaging is the provision of structural and functional information under physiologic conditions, mimicking the situation observed in the clinic. Molecular imaging can hasten drug development at the target identification and validation stages, in the synthesis and optimization of drug candidates and in pre-phase I to phase II clinical trials, i.e., at almost any point in the process. It provides the link between *in vitro* studies and those performed *in vivo*, in humans. Many fine reviews of the use of human imaging in drug development exist [2-10], and an entire issue of *The Journal of Clinical Pharmacology* has recently been dedicated to that topic [11], so this review will focus on the use of small animal imaging for that purpose. Hume *et al.* [12] and Myers [13] have recently reviewed small animal imaging with positron emission tomography (PET).

WHY SMALL ANIMAL IMAGING?

Small animal imaging includes mainly rodents, but also involves birds, snakes and other animals with a head or body diameter < 5 cm. Because they are accessible, easy to maintain, have a short reproductive cycle and, more recently, are easily genetically manipulated, the mouse remains the premier animal model for biomedical research. In the forty years since the discovery of the nude mouse, researchers have learned not only how to grow tumor xenografts orthotopically, but also to produce animals that develop tumors *de novo* or even fluoresce, at will. Approximately 25 million mice are used in biomedical research annually, representing over 90% of all mammalian studies [14]. Over 3,000 knockout strains are currently available and between knockouts, conditional knockouts, transgenic and mutant mice, there is essentially no limit to the diversity of strains able to be produced to study gene function. Perhaps the most obvious reason to image those mice is to learn about the effects genetic manipulation has on each strain, particularly since unexpected phenotypes arise. Imaging with x-ray computed tomography (CT), magnetic resonance (MR), ultrasound (US), optical and radionuclide techniques can provide a nearly complete phenotype, structurally, functionally and longitudinally, of a genetically altered animal. A main goal of such work currently is automation of that process. Other reasons to image (rather than dissect) mice are to decrease the number of animals needed per study, with concurrent decrease of statistical variance, since each animal may serve as its own control; to uncover biochemical pathways, *e.g*., signal transduction cascades and protein-protein interactions, as they occur *in vivo*, in mammals; and, to develop new diagnostic and therapeutic agents.

Small animal imaging began as merely another technique to answer questions posed in academic laboratories, but is rapidly becoming an industry. Several commercially available, miniaturized imaging systems for each modality and in-house molecular imaging capabilities are available at several pharmaceutical companies and equipment manufacturers worldwide. The National Cancer Institute (NCI) supports small animal imaging resource programs (SAIRPs), which are university-based and designed to augment ongoing biomedical research with imaging. Small animal imaging was initially undertaken on clinical imaging systems, from which much valuable information continues to be obtained, however it has become clear that to realize the full, i.e.,

*Address correspondence to this author at the Johns Hopkins University School of Medicine, Department of Radiology, 600 N. Wolfe Street, Phipps B-100, Baltimore, MD 21287-2182, USA; Tel: 410.955.2789; Fax: 410.614.1213; E-mail: mpomper@jhmi.edu

1381-6128/05 $50.00+.00

quantitative, potential of small animal imaging, dedicated scanners must be produced. Dedicated scanners are needed because the sizes of the regions to be imaged in small animals can be smaller than the resolution of clinical scanners, particularly for radionuclide applications; high-resolution imaging systems can be built with sensitivities on a par with clinical instruments; and, dedicated animal devices do not detract from clinical throughput and allow continuous laboratory investigation to proceed. That last point is actually the main reason that the first dedicated small animal radionuclide imaging device, the Hammersmith RATPET, was produced. Also, dedicated animal systems tend to be less expensive than their clinical counterparts (approximately 1/3 the price) and occupy less space. Although such dedicated systems tend to be housed in radiology departments, where adequate shielding from the high magnetic fields employed and proximity to a cyclotron are available, increasing use of commercially available ^{18}F-fluorodeoxyglucose (FDG) as a tracer, table-top optical imaging systems and portable ultrasound machines encourage the use of these imaging systems as standard laboratory equipment in any department concerned with molecular imaging research.

DRUG DEVELOPMENT: OVERVIEW

The most important step in the arduous process of drug development is target identification (Fig. **1**). Proteins mediate function and therefore are the primary targets in drug development. As we have entered the post-genomic era, the identification of therapeutic targets is no longer a bottleneck in the drug development process. Because of alternative splicing and post-translational modification of the 30,000-40,000 genes identified in the human genome, the number of potential targets is in the hundreds of thousands, up from the mere hundreds of potential targets under study before the sequence became available. Those potential targets must be prioritized so that the 10,000 or so that are clinically viable can be prioritized further and validated.

Target validation occurs through a number of proteomics methods including two-dimensional gel separation of protein mixtures followed by mass spectrometry (2D-MS), transcriptional profiling of mRNAs and functional screening [15]. High-throughput techniques are brought to bear at this stage, in analogy to small molecule screening but at the protein level. Biochemical screens for small molecule binding and enzymatic assays can be performed and have been automated on microarrays [16]. Antisense approaches can also be applied, where the gene that encodes the protein of interest can be shut off when the complementary oligonucleotide binds to its DNA sequence. Cellular function can then be assessed in the absence of function of that protein. An extension of that process to the *in vivo* case involves the use of knockout mice, where homologous recombination enables deletion of the gene that produces the protein of interest and

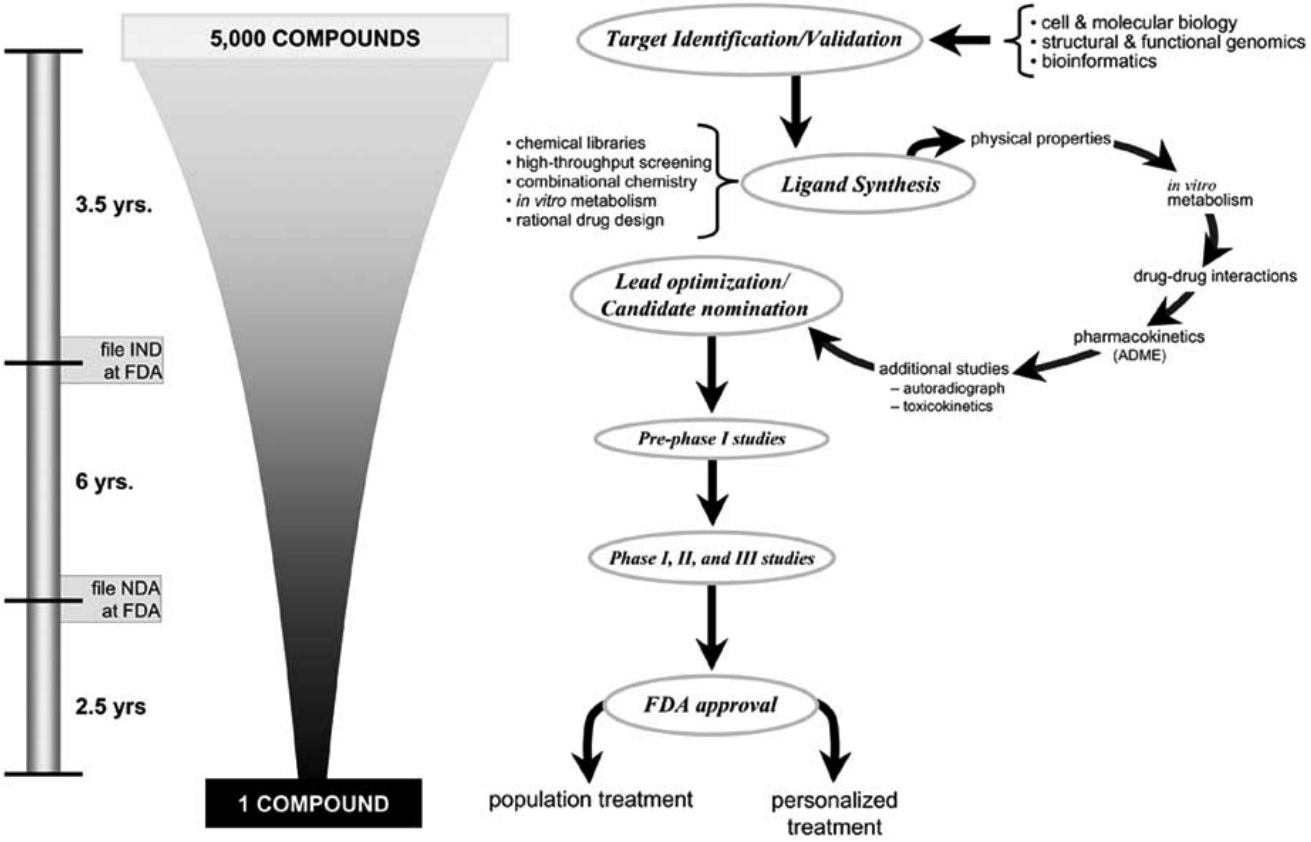

Fig. (1). Drug development.

the effects of the absence of function can then be determined in an animal model. Although surprising phenotypes occasionally arise, calling into question the validity of such models, their use remains a powerful, new method to assess protein function and is gaining increasing use not only in drug but also in radiopharmaceutical development [17]. Screening for the function of intracellular proteins employs protein-protein interaction mapping, a new technique that enables a better understanding of cellular events including signal transduction and drug susceptibility [15]. Phage display, in which a library of proteins can be analyzed on the surface of a bacteriophage, is another method to screen for protein-protein interactions [18, 19]. The mapping of protein-protein interactions is also a current goal in molecular imaging research [20, 21].

The target identification/validation stage is commensurate to the elucidation of pathophysiology of the underlying mechanism under study, *e.g*., apoptosis during development or cancer therapy, hypoxia-inducible factor-1 (HIF-1α) expression during hypoxia, or overexpression of the prostate-specific membrane antigen in prostate cancer. The vast number of new targets enables the development of therapeutic agents of unique specificity, such as imatinib mesylate (Gleevec), which takes advantage of the Bcr-Abl pathway in the treatment of acute leukemia [22]. For validation, those specific targets require specific functional assays, the most physiologically relevant of which are available through molecular imaging.

The screening of protein function can be avoided if the structure is known. Structure can be determined by nuclear magnetic resonance (NMR) spectroscopy or, more recently, through high-throughput x-ray crystallography, i.e., methods of structural genomics [23]. Homology modeling and computational docking methods also enable a guess at protein structure that, once known, permits the rational synthesis of suitable ligands. Pharmaceutical companies are turning to refined combinatorial libraries to find such ligands. Dynamic combinatorial chemistry and computer-assisted drug design are finding increasing use as well. Once compounds of acceptable affinity and selectivity are identified, their physical properties, i.e., solubility, pK_a, logP and passage through a monolayer of caco-2 cells, are determined. Each of those parameters is critical and can be a reason for failure of the drug candidate. Drug metabolism is then studied in human hepatocytes, if possible, or at least in hepatocytes of the species in which later toxicology studies will be performed. Drug-drug interactions are assayed and then the absorption, distribution, metabolism and excretion (ADME -- pharmacokinetics) of the candidate drug are determined in rodents and in other species. Further characterization involves radiolabeling the drug candidate and performing whole-body autoradiography and toxicokinetics, the correlation of changes in plasma and tissue concentrations with toxicity. At this point the drug candidate is ready to enter clinical trials.

Information from small animal imaging studies can be extremely helpful at the ligand synthesis/optimization stage, particularly in elucidating pharmacokinetics of the drug candidate. Pharmacokinetic imaging requires the drug candidate to be tagged in some way, usually radiolabeled, but increasingly with fluorescent labels and, for larger molecules, with magnetic labels. In almost all cases, except for radiolabeling an identical site in the drug candidate with carbon-11 for PET, one must be mindful that an analog, rather than the drug candidate, is being studied. Central nervous system (CNS) drugs can be tagged and tracked *in vivo* in a single animal to determine blood-brain barrier (BBB) permeability. Quantitative kinetic evaluation of drug candidates can be performed with PET, allowing calculation of relevant rate constants that describe tissue extraction, receptor-specific binding, nonspecific binding and/or enzyme turnover. Pharmacokinetic knowledge obtained from imaging enables continuous monitoring of the disposition of the drug candidate, not just snapshots of the plasma concentration of the unmetabolised component, which may have little relevance to the concentration of the drug candidate at the intended site of action. That is true of CNS drugs, where brain and plasma kinetics invariably diverge and for oncologic agents, where heterogenous tumor perfusion presents the lesion with an uneven or inadequate dose, not reflected in peripheral samples. Pharmacodynamic information, i.e., the effects of the drug candidate on the tissues, is also readily available through small animal imaging. Changes in blood flow critical to anti-angiogenic therapies can be assessed by PET, MR or US. Drug-drug interactions can be studied by radiotracers designed to probe the activity of multidrug resistance (MDR) pumps under the influence of MDR modulators, for example. All of that information can be used in an iterative fashion for structural refinement of lead compounds.

Phase I clinical trials consist of determining a safe dose of the drug candidate in healthy volunteers. Before that, i.e., in pre-phase I, radionuclide imaging has been applied in dose-finding exercises, particularly in CNS applications where receptor occupancy of drug candidates can be calculated [24]. Because only a small amount of mass is administered with radiotracers synthesized in high specific radioactivity, no pharmacologic effect from that administration results and doses as little as 1/1000 of the lowest initial dose in a phase I trial can be administered [6]. In phase II the drug candidate is administered to patient volunteers to evaluate efficacy and search for side effects. Effectiveness is further monitored in phase III, as is the presence of long-term side effects. Preclinical development takes an estimated 3.5 years while about 6 years are required for clinical trials needed to apply to the FDA for a new drug application (NDA). A further 2.5 years is required for that application to be approved (Fig. **1**). In all, about one in 5,000 drugs reaches that stage, at a cost of up to $700 million.

Imaging endpoints included in clinical trials, such as the RECIST (Response Evaluation Criteria in Solid Tumors) criteria, rely on anatomic changes to assess the efficacy of antitumor drugs, with progression defined as a 40% increase in tumor volume [25]. But physiologic changes detected with molecular imaging techniques antedate anatomic changes and should be more sensitive in assessing efficacy. Accordingly PET is being applied increasingly for therapeutic monitoring, particularly for cancer, where new agents may be merely cytostatic, having a minimal effect on lesion size [26]. One problem in using physiologic endpoints in determining efficacy is the lack of standardization of techniques of data acquisition and analysis, which, in the case of clinical

PET, extend from measuring the standardized uptake value corrected for body surface area (SUV_{BSA}) to full kinetic modeling. Agents other than FDG, such as 3'-deoxy-3'-[^{18}F]fluorothymidine (FLT) [27], an agent to image cell proliferation, and MS-325 (AngioMARK) [28], a blood pool MR contrast agent, are beginning to see clinical use, the latter in phase III trials. Although those agents are able to be tested in humans directly, input from small animal imaging during early clinical trials can refine the imaging protocols and answer unforeseen questions related to pharmacokinetics, *e.g.*, because performing animal studies is much more efficient. A new criterion for predicting efficacy of a drug candidate will be to see if the degree of modulation of an imaging probe in an animal model that is associated with activity is obtained with human imaging, rather than ensuring only that adequate plasma concentrations are achieved [2].

The relevance of rodent models of human disease is occasionally questioned because species differences in drug candidate metabolism, often by cytochrome-P450 enzymes, exist [29]. As mentioned above, knockout mice are always phenotypically heterogeneous, suggesting caution in extrapolation to human disease. Orthotopic xenograft models attempt to provide a more physiologic microenvironment for tumors but that microenvironment remains largely murine, and the utility of orthotopic models has probably been overstated except for select cases [30]. Nevertheless the rodent models provide the best first guess at drug candidate pharmacokinetics and effects, provided that correlation with standard biochemical markers is obtained and species differences are accounted for when necessary.

LOGISTICS OF SMALL ANIMAL IMAGING

Small animal imaging studies are currently not high-throughput procedures. An MR perfusion study of a mouse tumor, with preparation, takes about as long as the comparable clinical study. If live studies are intended, small animals must generally be anesthetized to undergo imaging. Anesthesia, whether inhalational or administered by injection (intraperitoneal or intramuscular), is an important confound in animal imaging experiments, particularly for imaging CNS and cardiovascular phenomena, where the effects of anesthesia on blood flow and metabolism are often greater than the signal from the underlying biology of interest. Creative efforts to image awake, mildly or unrestrained animals are underway, but the vast majority of studies employ anesthesia. The choice of anesthesia regimen depends on the underlying question. There are regimens that have less effect than others on vascular and metabolic changes that occur with brain activation, *e.g.*, alpha-chloralose (injection) and nitrous oxide/isofluorane (inhalational). The degree of inhalational anesthesia can be controlled during an imaging study, representing a distinct advantage to anesthetics that are injected; however, use of volatile anesthetics requires expensive equipment and training. Mouse strains have varying sensitivities to anesthesia, usually uncovered empirically, that must also be taken into account [31]. Custom-designed, multimodality-compatible imaging chambers exist for small animal imaging, although these devices have not been standardized nor have they become commercially available. Details of small animal anesthesia induction and maintenance, physiologic monitoring, catheterization and assuring adequate warmth, including during imaging, have been addressed in detail previously [31-34].

Once adequate anesthesia and physiologic monitoring are assured, a new set of challenges arises, depending on the biological information sought and modality employed. For example, two major sources of error include motion and partial volume/spillover for MR and radionuclide applications, respectively. Cardiac gating becomes challenging in animals with heart rates of nearly 400 beats/minute that undergo high-resolution (< 0.03 mm^3) imaging, but stethoscopes developed for that purpose have been developed [35]. Partial volume correction and spillover of radioactivity in regions of interest (ROI) on PET images is only beginning to be evaluated in human PET studies, let alone in small animal imaging. Despite sophisticated gating mechanisms and monitoring, breathing can be erratic, in part due to the configuration of the mouse thorax; position of the animal becomes relevant during prolonged imaging sessions. Those and other challenges are detailed below in the context of the modalities that serve small animal imaging.

SMALL ANIMAL IMAGING IN DRUG DEVELOPMENT: EXAMPLES BY MODALITY

The same modalities available in the clinic are scaled down in dedicated devices to accommodate small animals. That holds true for all modalities, including some optical techniques. Scaling down of each modality to serve small animals is an important issue, because careful knowledge of the scaling factors involved, which are not necessarily linear, is necessary to assure an appropriate experimental design. The modalities are complementary in information, vary in anatomic and temporal resolution, sensitivity, cost and other factors, as previously described [36]. Table **1** synthesizes those factors as they apply to drug development. Several generalizations are possible: contrast agents enhance the utility of all modalities; CT and MR are used primarily for anatomy and pharmacodynamics; US is used for pharmacodynamics of vascular agents; and, optical and radionuclide agents image gene expression, enzymes, receptors and transporters. The sensitivities of the systems for detecting molecular events, of paramount importance in drug development, can roughly be described as: optical > radionuclide >> MR > US ≥ CT. Radiopharmaceuticals are the largest and most chemically diverse group of molecular imaging agents. All modalities are eminently translatable from small animals to the clinic.

COMPUTED TOMOGRAPHY (CT)

CT is the two- or three-dimensional reconstruction of x-ray data. Structures of different density, i.e., bone, soft tissue, fat and air, are resolved by x-ray imaging. The goal behind CT, as with all tomographic techniques, is to provide internal structure. Small animal CT scanners, which are commercially available [37], can play an important role in drug development by providing an anatomic context for the disposition of functional imaging agents. Mutual information algorithms have been developed to overlay anatomic and functional imaging information using CT and PET (Fig. **2**).

Table 1. Small Animal Imaging Modalities

Modality	Uses in drug development
X-ray computed tomography (CT)	• phenotyping • vascular therapies (pharmacodynamics) • lung tumor and bone disease models
Magnetic resonance Imaging ❑ imaging (MRI) ❑ microscopy (MRM) ❑ spectroscopy (MRS) ❑ functional MRI (fMRI) ❑ dynamic contrast-enhanced MRI (DCI-MRI) ❑ diffusion-weighted MRI (DWI) ❑ amide proton transfer imaging (APT-I)	• phenotyping • vascular therapies (pharmacodynamics) • assessing cellular metabolism (pH, pO_2, lactate, and other species -- pharmacodynamics) • pharmacokinetics of isotopically labeled drugs • cell tracking • gene expression • drug delivery • receptor-based imaging (?)
Ultrasound (US) ❑ imaging ❑ biomicroscopy ❑ contrast-enhanced ❑ targeted ○ passive ○ active	• phenotyping • vascular therapies (pharmacodynamics) • drug delivery
Optical ❑ fluorescence- mediated tomography (FMT) ❑ bioluminescence imaging (BLI) ❑ coherence tomography (OCT)	• therapeutic monitoring (infection and cancer) • gene expression • cell tracking • receptor-based imaging • activatable probes for enzyme activity • validation of radionuclide reporters • protein-protein interaction
Radionuclide ❑ planar gamma scintigraphy ❑ single photon emission computed tomography (SPECT) ❑ positron emission tomography (PET)	• pharmacokinetics (small molecules→ macromolecule probes) • pharmacodynamics • gene expression • cell tracking • protein-protein interaction • receptor-based imaging

Scanners that obtain anatomic and functional information concurrently, i.e., PET/CT devices, have been clinically available for two years, although no such device is yet available for small animal imaging. Small animal CT scanners produce images at resolutions comparable to those of MR imaging (50 μm), particularly with contrast administration [37]. Data acquisition takes anywhere from 5 to 30 min, depending on the level of resolution needed. Because of high anatomic resolution, CT can be used in phenotyping genetically manipulated animals. The radiation dose delivered for such a screening study is estimated to be on the order of 5% of the LD50/30 for mature mice, which is a significant value, suggesting that longitudinal study protocols must be carefully designed.

Small animal CT has been used to study lung tumors [38], bone mineral density during parathyroid hormone treatment [39] and vascular endothelial growth factor (VEGF) stimulation of bone repair [40], but its greatest contribution to drug development will be in studying the microvasculature, in analogy to MR. Iodinated contrast agents have been used in rodents to visualize the renal vascular tree and other aspects of the microcirculation [41]. Blood pool contrast agents consisting of iodine-substituted poly-L-lysine micelles [42] or iopromide-carrying liposomes [43], *e.g.*, are being developed for small animals. High-resolution functional CT can be performed in rodents using a clinical scanner. Charnsangavej *et al.* [44] studied the response of murine mammary tumors, transplanted to Fischer rats, to SU-5416,

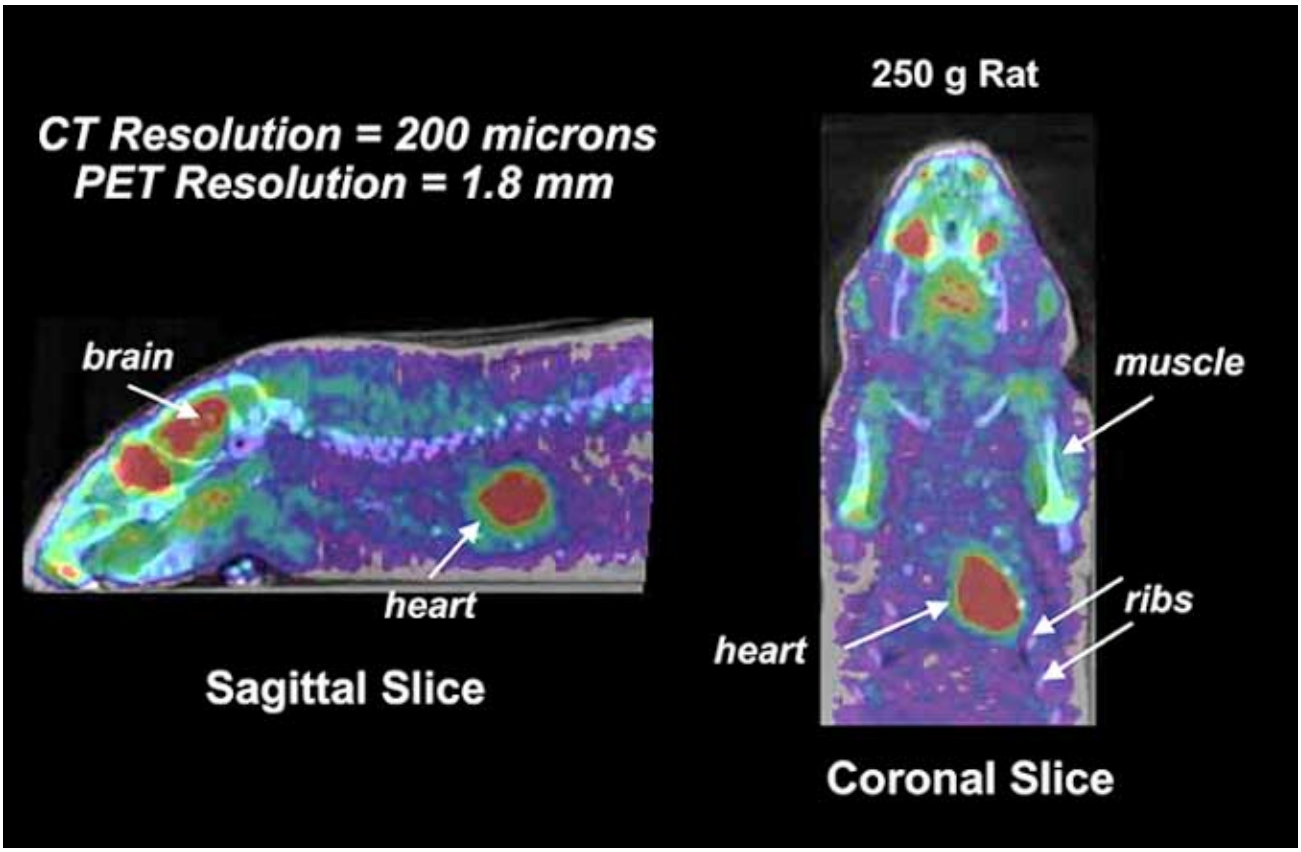

Fig. (2). Registered ATLAS FDG-PET and CT images [courtesy: Michael Green, NIH Clinical Center].

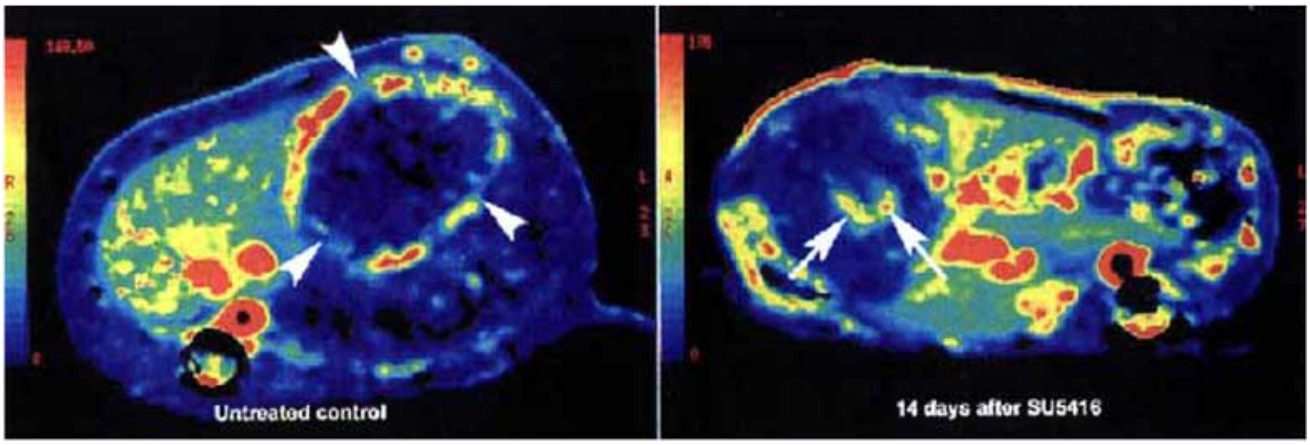

Fig. (3). Functional CT blood flow maps. Arrows indicate tumor before and after 14 days of treatment with SU5416, an anti-angiogenic agent, in the liver of rats [44].

an anti-angiogenic agent (Fig. **3**). They reasoned that because anti-angiogenic therapy is cytostatic rather than cytotoxic, conventional means by which to measure tumor response, i.e., anatomic shrinkage, are irrelevant. With functional CT, quantification of blood flow (BF), blood volume (BV), mean transit time (MTT) and permeability surface (PS) parameters is possible. To validate those parameters they performed cine-CT and compared them to the findings on histological examination (vessel count). Surprisingly, there was no change in BF, BV and PS between treated animals and controls, but there was redistribution of the vasculature, with higher flow within the center of the treated tumors. That finding has important implications for access of chemotherapeutic agents to treated tumors, suggesting the need for combination therapy to supplement anti-angiogenesis. Because of the absence of radiation, exquisite soft tissue resolution, higher sensitivity to a wide variety of contrast agents and flexible operating parameters of MR, CT will likely remain secondary for dynamic vascular indications.

MAGNETIC RESONANCE (MR)

MR tissue characterization relies on the detection of water protons through the application of radiofrequency pulses to the animal in a magnetic field. Differences in the microenvironment of those protons between tissues determine the appearance of the image. The microenvironment might contain a higher density of protons or a chemical and physical structure that may be more or less permissive for rapid longitudinal (T_1) or transverse (T_2) relaxation of protons. MR imaging sequences can also be programmed to emphasize the ability of water to diffuse throughout the tissue, a functional aspect of the technique, as shown in equation 1, where S is MR signal intensity, N(h) is proton density,

$$S = N(h) * (1-\exp(-TR/T_1)) * \exp(-TE/T_2) * \exp(-bD) \quad \text{[eq. 1]}$$

and the remaining three terms indicate T_1 relaxation, T_2 relaxation and diffusion, while b is the diffusion gradient factor and D is the diffusion coefficient. Researchers dedicated the first two decades of MR imaging research to refining the acquisition of anatomic images by developing more efficient pulse sequences that delivered images of increasing soft tissue resolution while the last decade has been concerned with exploiting the functional capabilities of MR.

Applying small, specialized coils, high magnetic fields and high-powered gradients enables resolution on the order of 50 μm and even 20 μm for isolated organs for MR microscopy (Fig. **4**). Most clinical MR imaging occurs in magnetic fields of 1.5 Tesla (T) whereas small animal imaging can be performed at 11.7 T and higher. The increase in magnetic field in going from humans to mice improves the volumetric resolution, for an imaging voxel, from 80 mm^3 to approximately 7.3 mm^3 [33]. Such high-resolution imaging lends itself perfectly to mouse phenotyping, but the functional aspects of MR imaging are of greater immediate relevance to drug development. The high magnetic fields available for small animal imaging also benefit MR spectroscopy (MRS), where spectral resolution is improved allowing more accurate quantification of chemical species within tissue.

Tumor Microenvironment

Most applications of small animal MR imaging to drug development are for antineoplastic agents, primarily because an emerging sub-field within functional MR research focuses on the physiology of the tumor microenvironment. Researchers in that new sub-field use MRS to assess tumor pH and oxygen status in addition to the metabolites that can be measured by proton and other nuclear (^{23}Na, ^{31}P, ^{19}F, ^{13}C) MRS [45]. Because of the heterogenously and inefficiently perfused tumor milieu, tumors tend to be hypoxic and support an acidic pH. It is hypothesized that such a milieu promotes local invasion and metastases of tumors. Chemotherapy intended to halt those processes must therefore address those conditions. For example, weakly basic drugs such as the anthracyclines likely become compartmentalized within heterogeneous interstitial regions due to the low pH within tumors, detracting from their effectiveness [45]. The lack of adequate perfusion has important implications for the pharmacokinetics of antineoplastic agents, i.e., they may never reach their targets. Larger agents, such as therapeutic antibodies, are particularly at risk due to the suggested increased interstitial pressure within tumors that are already poorly perfused [46]. The low oxygen tension within tumors has negative implications for radiotherapy as well, which relies on the production of free radicals and other reactive species derived from oxygen upon interaction with ionizing radiation. The development of radiosensitizers may benefit from an understanding of the tumor microenvironment [47, 48].

Tumor hypoxia is measured by gradient echo MR techniques (GRE-MR) that are sensitive to small changes in magnetic susceptibility that occur in response to the presence of oxygen. Oxygenated hemoglobin (oxyhemoglobin) is nonparamagnetic, and will therefore exert no effect on a magnetic field, while deoxyhemoglobin is paramagnetic and will. Specifically, deoxyhemoglobin will cause a decrease in

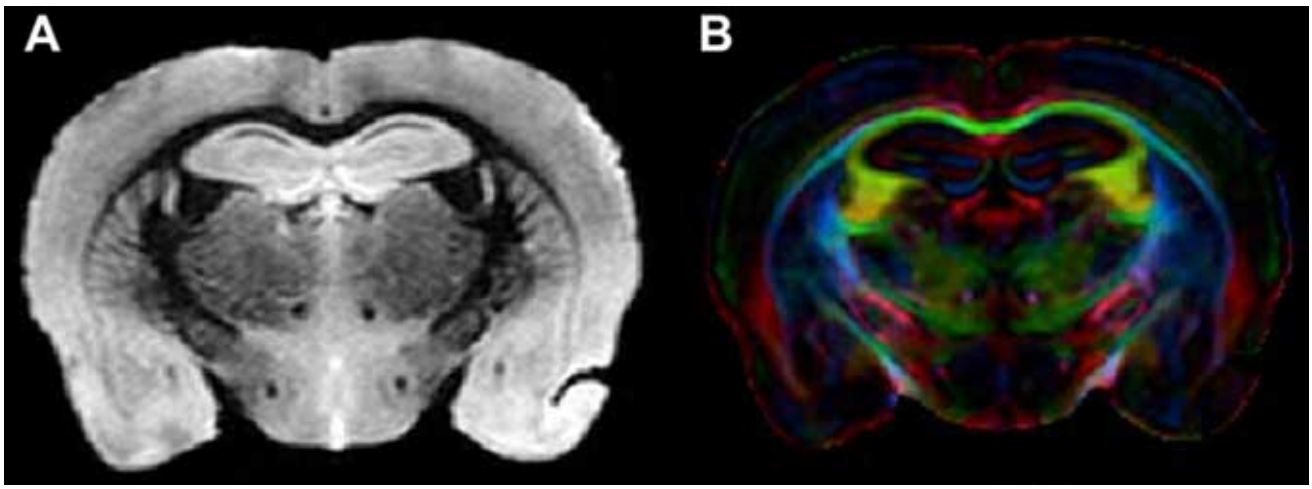

Fig. (4). High-resolution mouse MRI (A) and fiber tracking (B) [177].

signal intensity by shortening the apparent transverse relaxation time (T_2*). Contrast is therefore generated according to a blood oxygen level dependent (BOLD) mechanism. Key to techniques that rely on BOLD to generate contrast is the necessity to compare a resting and an activated state. BOLD is the underlying mechanism for functional MR imaging (fMRI) that is used in the clinic for brain mapping. In addition to somatosensory stimulation or merely thinking, other activation paradigms involve pharmacologic challenges, which have utility outside of the CNS. Carbogen, a 95:5 mixture of oxygen and carbon dioxide, is used in tumor imaging to induce hyperoxygenation that can be detected by GRE-MR. Physiologic challenges, including the administration of vasoactive drugs, can then be studied with MR. Brain activation with pharmacologic agents has been described as pharmacological MRI (phMRI), and has been applied in humans to study the effects of analgesics and other centrally acting agents on blood flow [49, 50]. The assessment of hemodynamic changes evoked by diltiazem, a calcium-channel blocker, in a murine Ehrlich ascites tumor model is another example [51]. Diltiazem, by increasing tumor blood flow, is proffered as a radiosensitizer. Shaharabany *et al.* imaged the hepatocyte growth factor scatter factor (HGF/SF)-mediated activation of the Met tyrosine kinase growth factor receptor system *in vivo*, using BOLD-MRI [52]. Met is a viable target for drug discovery because it is implicated in the pathogenesis of a variety of human epithelial cancers [53].

^{19}F-MRI can also be used to study tumor oxygen tension due to the high solubility of oxygen in perfluorocarbon emusions. That technique can be used to follow therapeutic interventions designed to increase oxygen delivery to tumors. Intracellular tumor pH is measured by the chemical shift changes of endogenous inorganic phosphate by ^{31}P-MRS, often with the help of an indicator, 3-aminopropyl phosphonate (3-APP), by ^{1}H-MRS, ^{19}F-MRS, contrast-enhanced MRI or magnetization transfer [43, 54].

MR Spectroscopy/Spectroscopic Imaging

In terms of measuring absolute concentrations of various metabolites, it is only the endogenous metabolites such as choline, creatine, *N*-acetylaspartate, lactate, glutamate and several others that are in sufficient concentration (on the order of 1-10 m*M*) to be detected and imaged (MR spectroscopic imaging – MRSI [55]) with a reasonable degree of resolution using ^{1}H-MRS (Fig. **5**). It is the rare case when an exogenously administered small molecule (< 500 Da) can be interrogated and analyzed pharmacokinetically with MRS, because of the high concentration required, which often leads to pharmacological effects including toxicity. Nevertheless, the intratumoral conversion of 5-fluorocytosine to 5-fluorouracil has been studied in that fashion [56], as have the kinetics of ^{13}C-glucose in cats, [57]. To predict the delivery of chemotherapeutic agents to tumors, Artemov *et al.* [58] correlated the delivery of a standard MR contrast agent, gadolinium-diethylenetriaminepentaacetic acid (GdDTPA),

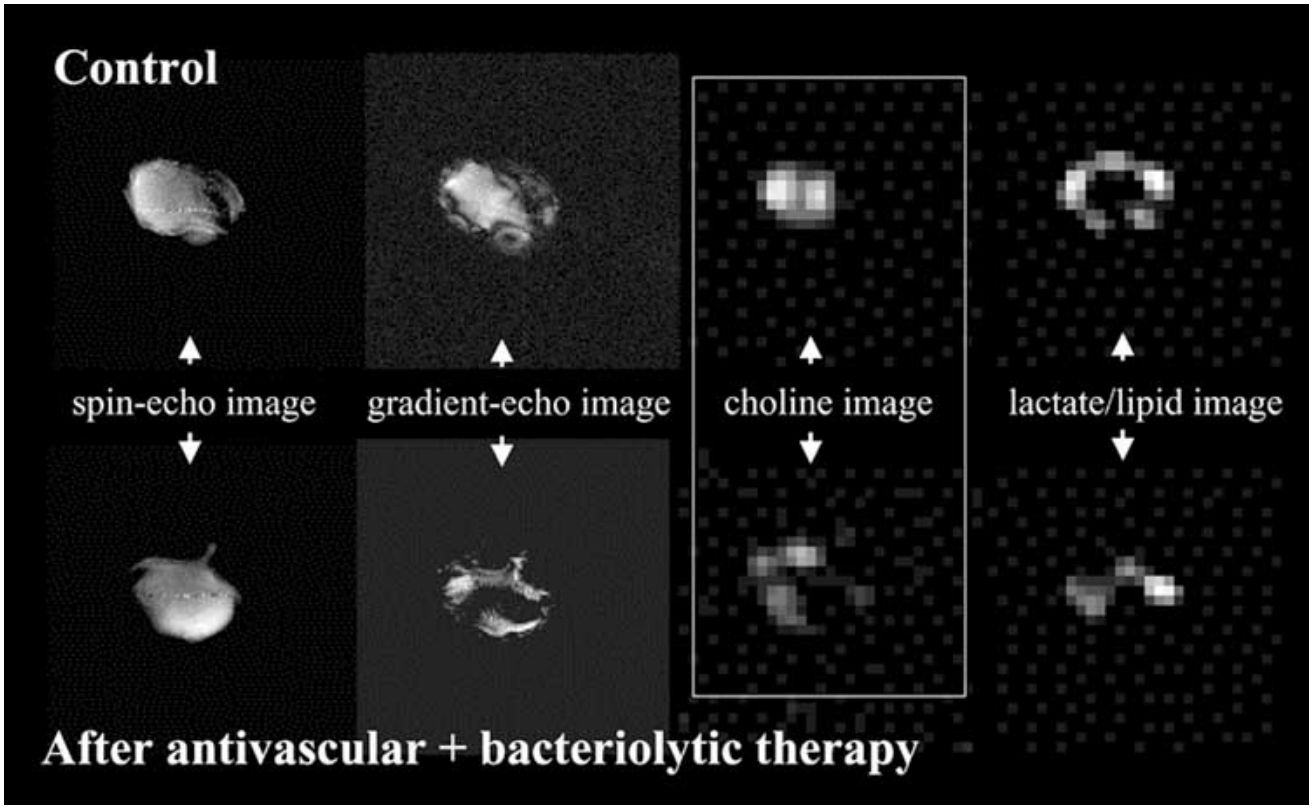

Fig. (5). ^{1}H-MR Spectroscopy. Note the decrease in choline, a marker of cell turnover, in colon cancer xenografts in SCID mice after experimental (anti-vascular + bacteriolytic) therapy [courtesy: Zaver Bhujwalla, Johns Hopkins University].

with that of an isotopically labeled tumor differentiating agent, ^{13}C-phenylacetate. They found a high correlation between the delivery of the two agents, although retention did not correlate. That experiment has implications for using MR contrast agents that mimic the size, weight and lipophilicity of therapeutic agents to predict delivery of those therapeutic agents to the site of interest.

Perfusion Imaging

Perfusion MR imaging is a clinical technique useful for therapeutic monitoring in a variety of diseases that affect blood flow, including myocardial infarction [59], stroke [60], organ transplantation [61], and cancer, [62]. The response to pharmacological challenge can also be measured with perfusion MRI [63]. Perfusion can be measured using contrast enhancement (dynamic contrast-enhanced MRI – DCE-MRI) or though arterial spin labeling, where a bolus of ingoing blood is magnetically tagged as an endogenous contrast agent [64]. Pharmacokinetic models for describing the disposition of contrast agents such as GdDTPA have been derived [65, 66]. In addition to clinical application, perfusion MR can be used to uncover mechanisms of pathogenesis, *e.g.*, in cancer. Using albumin-GdDTPA, a blood pool MR contrast agent, Bhujwalla *et al*. [67] studied a series of breast and prostate tumors of differing metastatic potential to demonstrate that areas of high vascular volume within the tumors were not spatially equivalent with areas of high permeability where tumor necrosis predominates, a finding with implications for the delivery of macromolecular therapeutic agents. That group has also used perfusion MR imaging and combined vascular volume/permeability maps to monitor the response of the MATLyLu rat model of metastatic prostate cancer to the angiogenesis inhibitor TNP-470 (Fig. **6**). Redistribution of permeability to the surface of the tumor was noted upon treatment. Su *et al.* [68] used DCE-MRI to study the effect that gene therapy (*e.g*., IL1-α) had on altering the vasculature of a rat C6 glioma model, and found that the changes in vascular volume preceded those in tumor volume. Evelhoch studied the effects of ZD6126 (*N*-acetylcolchinol-O-phosphate), a prodrug for *N*-acetylcolchinol, in murine adenocarcinoma C38. *N*-Acetylcolchinol disrupts the tubulin cytoskeleton of neoendothelial cells causing vascular occlusion. They detected the spatial distribution of dose-dependent vascular effects of that agent that were apparent within 24 hours of single-dose treatment, with no change in tumor size (Fig. **7**).

Diffusion-Weighted Imaging

Diffusion-weighted MR imaging (DWI) relies on the directionality of motion of water in tissue that can be detected upon using a motion-dependent MR pulse sequence. When appropriately-timed magnetic field gradients are applied to the sample, a diffusion-weighting term enters the equation describing signal detected in an MR study (equation 1). Diffusion of water through tissue is random, the speed and direction of which is dictated by the presence of barriers, such as macromolecules, cell membranes and cellular organelles. Being random, diffusion occurs isotropically; however, because of the organization of certain tissues, *e.g*., white matter tracts or sheets of tumor cells in the brain, diffusion may be anisotropic or directional. Clinically, DWI is used most frequently in conjunction with perfusion imaging in the context of acute stroke, where a mismatch between the spatial distribution of abnormalities on the two sets of images, i.e., larger perfusion than diffusion "defect", might suggest therapeutic intervention (thrombolytics). DWI may contribute to tumor imaging in two ways: in the differentiation of infiltrating tumor from vasogenic edema and in tumor grading [69]. Chenevert *et al.* have recently reviewed the use of DWI in brain tumor monitoring, both in

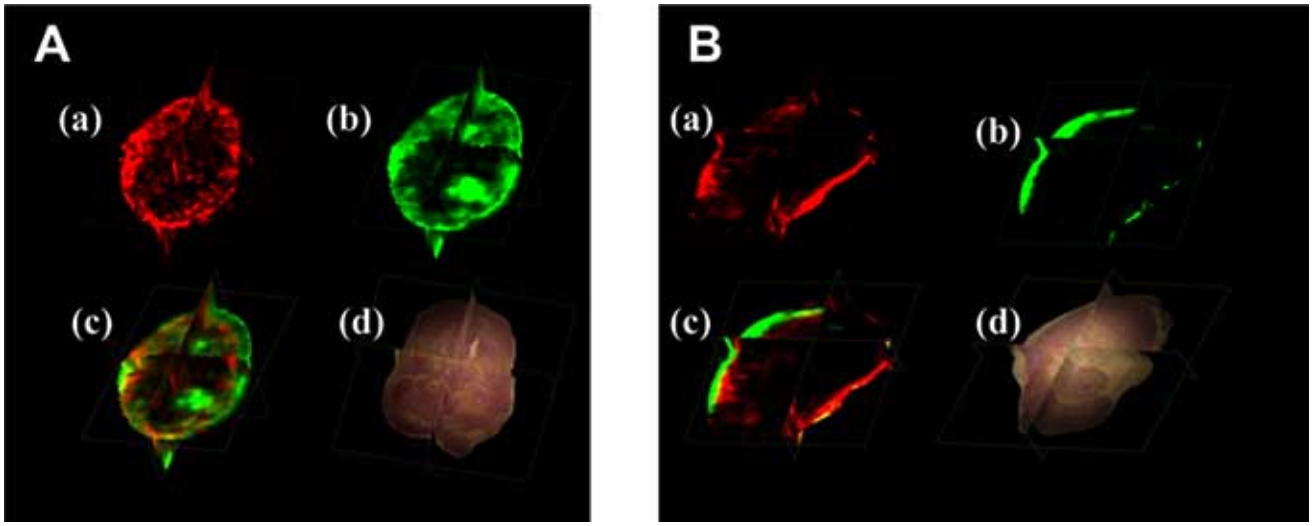

Fig. (6). Vascular MR imaging. Triplanar view of 3D reconstructed maps of (a) vascular volume (b) permeability, (c) combined vascular volume and permeability and (d) hematoxylin and eosin stained sections of a MATLyLu tumor (volume 405 mm^3) before (A) and after (B) treatment with TNP-470. Note peripheral redistribution of permeability upon treatment [Courtesy: Zaver Bhujwalla, Johns Hopkins University].

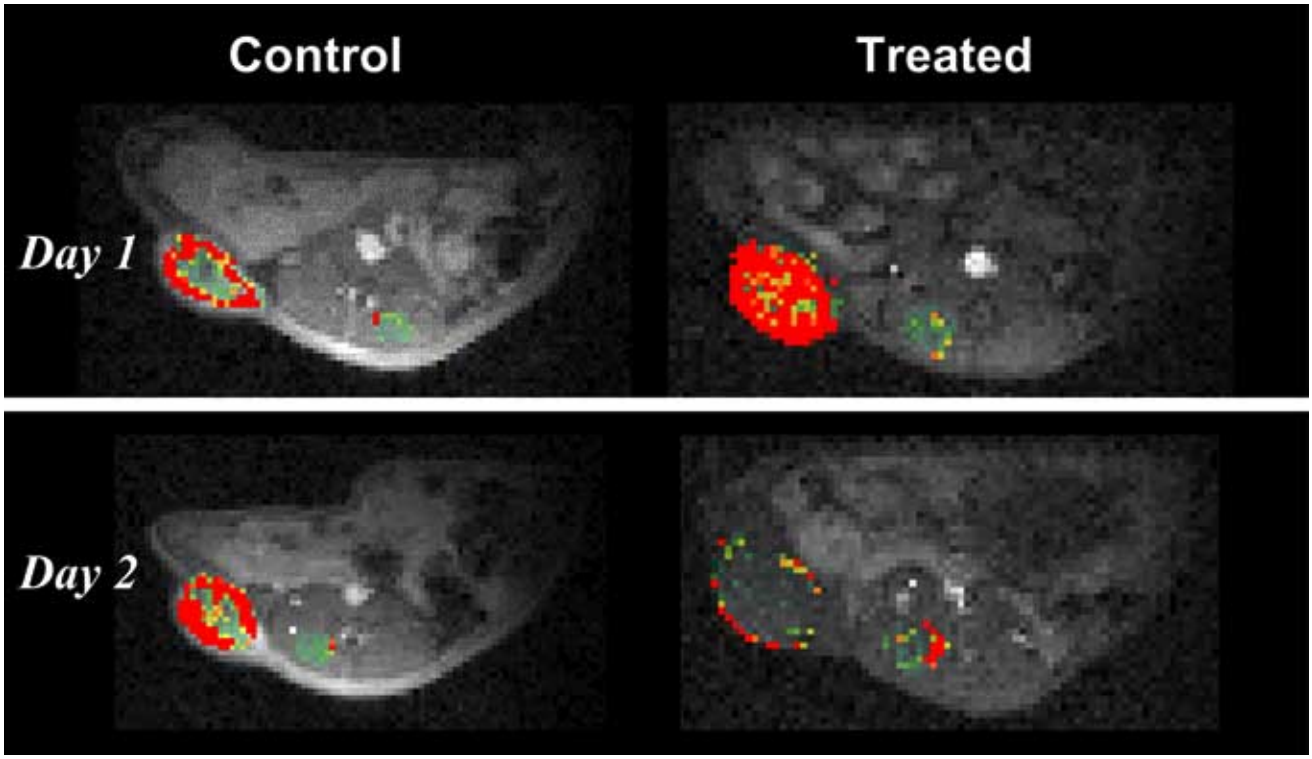

Fig. (7). Anti-vascular therapy (ZD626). Note redistribution of flow to tumor periphery with treatment [courtesy: Jeff Evelhoch, Pharmacia Corporation].

human subjects and small animals [70]. The underlying principle for therapeutic monitoring is that as tumors succumb to treatment, they become smaller as their cell membranes become permeable to water. Fewer barriers to water diffusion exist, so the apparent diffusion coefficient (ADC) will increase in effectively treated tumors. Changes in ADC are evident before changes in tumor volume detected by conventional means.

New Applications

The potential for functional MR techniques in drug development is further illustrated by a number of highly creative, new applications. Aspects of the hostile tumor microenvironment including decreased pH and oxygen tension can drive gene expression, evoking activation of genes necessary for cell survival under such conditions [45]. In particular, low oxygen tension upregulates expression of HIF-1α, which then dimerizes with HIF-1β to form a transcription factor that binds to downstream, specific hypoxia response elements (HREs) in DNA including the genes coding for VEGF and Glut-1. Raman *et al.* allowed PC-3 prostate tumors transfected with the HRE for VEGF to grow until the central core became hypoxic. Using an HRE-GFP construct they demonstrated activation of the HRE through optical imaging that was co-registered with vascular volume and permeability maps. The maps showed areas of low volume and high perfusion in the region of high HRE expression, as expected, since VEGF is believed to be a marker for vascular permeability [67].

Louie *et al.* used cleavable MR contrast agents to image gene expression *in vivo* [71]. In their scheme, the agent was synthesized in such a way to shield Gd from water, preventing its T_1-lowering (and signal enhancement) effect. Once in the vicinity of an enzyme of choice, in their case β-galactosidase, the agent was cleaved (hydrolyzed) in a site-selective process revealing Gd and therefore signal enhancement. That group has also developed calcium-sensing MR contrast agents [72]. Those agents are fraught with poor cellular penetrability and may have limited utility for probing intracellular events noninvasively; however, that hurdle may be overcome by synthesizing more lipophilic agents or agents linked to the HIV-1 Tat protein, which can effect rapid cellular penetration of macromolecular species [73].

MR is a relatively insensitive technique for detecting chemical species and receptors *in vivo* [74], with concentrations down to 10-100 μ*M* detectable with relaxivity-based agents. A variety of methods to increase that sensitivity have been undertaken, including the use of contrast agents that have been functionalized with biotin-GdDTPA chelates [75], superparamagnetic, iron-containing particles, magnetodendrimers [76] and saturation transfer of cationic polymers [77]. Those techniques have been used in imaging gene expression and cell tracking in small animals. In preliminary studies Artemov *et al.* demonstrated receptor-specific MR imaging at HER-2/neu sites in tumors overexpressing that protein using biotin-GdDTPA linked to anti-HER-2/neu (herceptin)-avidin (Fig. **8**). Signal amplification is present in that system because there are several GdDTPA per monoclonal antibody (MoAb). MoAb-mediated MR imaging may be difficult to scale up from mice to larger animals due to the increasing difficulty of saturating the target sites as the species size increases [74].

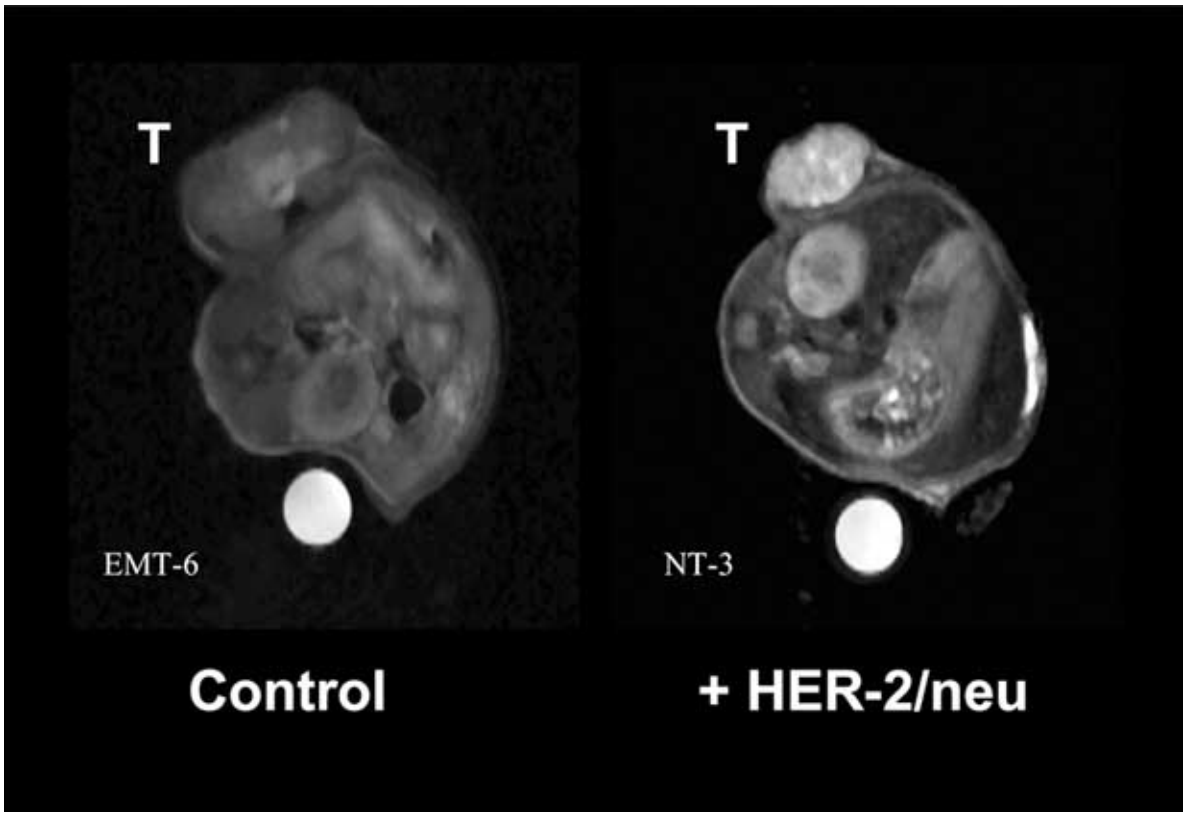

Fig. (8). MR Receptor Imaging. T_1-weighted images were obtained 22 hrs after administration of a targeted contrast agent (anti-HER-2/neu-GdDTPA). Note high uptake of contrast agent in cells transfected with HER-2/neu (NT-3). Tumors are demarcated by T with a bright phantom at the bottom of image [courtesy: Dmitri Artemov, Johns Hopkins University].

Signal amplification is the hallmark of Weissleder's method to image the expression of the transferrin (Tf) receptor gene with monocrystalline iron oxide particles conjugated to Tf (Tf-MION) [78, 79]. In that instance tumors transfected with an engineered Tf receptor internalize Tf-MION while those without the gene do not. The receptor was engineered such that the normal mechanism of down-regulation of Tf internalization upon Tf binding was removed. Since the Tf receptors are recycled to the cell surface continually, many Tf-MION conjugates may be internalized, amplifying the (negative) signal. That represented the first example of MR imaging to visualize gene expression. As with other imaging reporter systems to be discussed, the significance lies in its generalizability, i.e., that one may link the promoter of a gene of interest to expression of Tf receptor, which can be imaged, effecting an indirect measure of expression of the desired gene (Fig. **9**). The reporter protein can be internal, such as the enzyme HSV1-TK (used for PET), or it can be on the cell surface, such as Tf receptor (MR) or the dopamine D_2 receptor (PET). In those examples the reporter probes can be 9-[4-[^{18}F]fluoro-3-(hydroxymethyl)butyl]guanine (^{18}F-FHBG), Tf-MION and ^{18}F-fluoroethylspiperone, respectively. Dual modality reporter systems, *e.g.*, that produce GFP and HSV1-TK concurrently, have been developed for cross-modality correlation [80].

Therapeutic agents that rely on cell tracking will benefit from being able to image cell migration in small animals. Initial applications of that technology are in immunological and transplantation research and in following the course of stem cell therapies to reconstitute aspects of the CNS [81-85]. Bulte has used that technique to follow oligodendrocyte progenitor cells transplanted within the rat spinal cord in an experimental model of multiple sclerosis (Fig. **10**) [86].

Goffeney has developed a new way to enhance the sensitivity of MR imaging by factors of 5 x 10^5 using a technique called amide-proton transfer imaging (APT-I) [77]. The rationale for the development of APT-I was to be able to image directly cationic polymers that can be used as vectors for gene therapy. The technique can be extended to any molecule that contains a large number of amide protons, such as might be present in new blood pool MR contrast agents or drug delivery vehicles. APT-I takes advantage of the exchangeability of water and amide protons in solution (or tissue). As stated above, the MR signal emanates from water protons. One may indirectly gauge the concentration of species that are in exchange with those protons if they are in sufficient number and resonate at the appropriate frequency. The amide protons of poly-L-lysine are optimal for demonstration of the technique. By irradiating a sample containing poly-L-lysine, which contains 2,332 amide protons, at the amide proton frequency, one may decrease the signal intensity of the image by transferring the saturation of the N-H signal to H-O-H, which is imaged directly. A preliminary application of that technique to study ischemia in the rat brain at 3 T is shown in Fig. **11**.

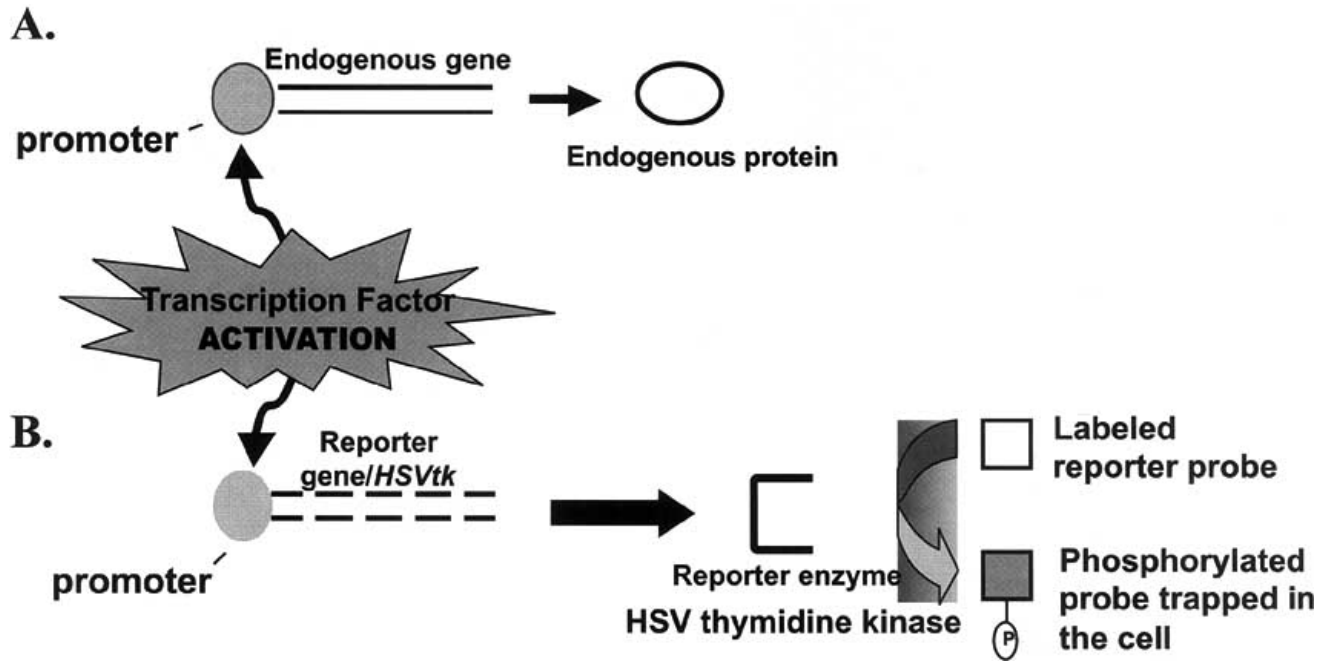

Fig. (9). Gene reporter/probe concept. Transcription of the reporter protein is linked to that of a gene of interest. The reporter may be intracellular (*e.g.*, an enzyme such as HSV1-TK) or it may be on the cell surface (*e.g.*, Tfr). The degree of transcription of the gene of interest (product not imageable) can be inferred because it and the gene encoding the reporter protein (product imageable) are transcribed in a 1:1 stoichiometry.

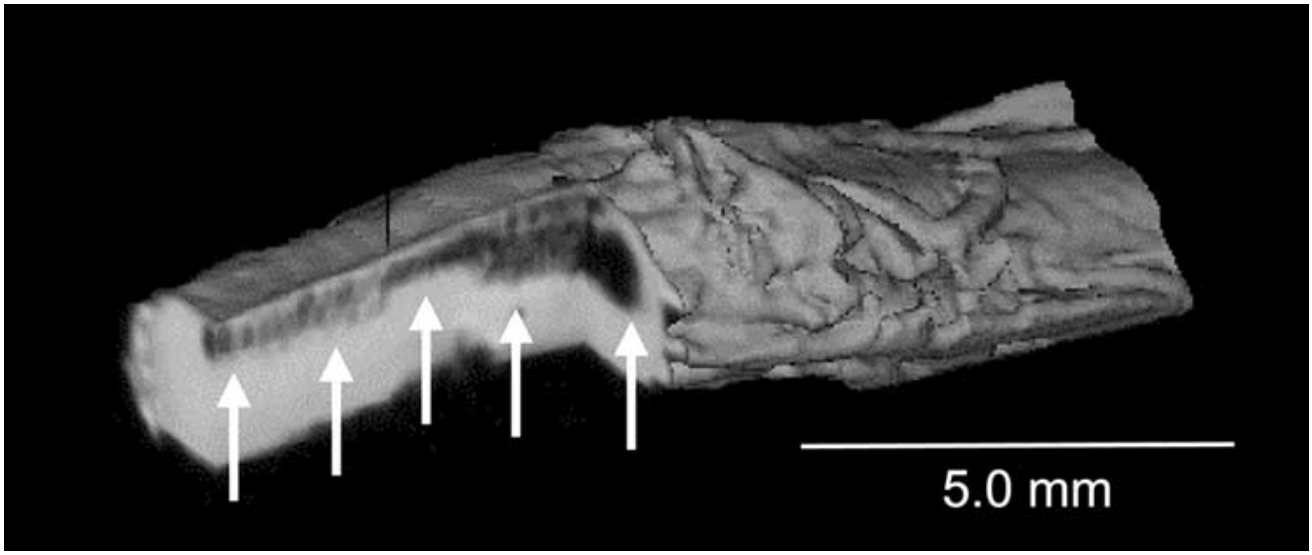

Fig. (10). Stem cell tracking. Magnetically labeled oligodendrocyte progenitors are tracked over time in rat spinal cord (arrows) [86].

ULTRASOUND (US)

US relies on the emission and detection of sound waves that are altered by traveling through tissue. Different tissues have different acoustic signatures. Imaging with US has become a mainstay of rapid clinical diagnosis. Its application to small animals has not been as extensive as the other modalities, nevertheless recent advances in US biomicroscopy, i.e., high-frequency (20-200 MHz) imaging, targeted contrast agents and US-mediated drug delivery promise to enhance the use of US in small animal imaging in the future [87]. As with CT and MR, the majority of US applications to drug development will be in detecting changes in the vasculature during therapy with, *e.g.*, anti-angiogenic agents. An advantage that US has over those other modalities in that regard is the fact that US contrast agents remain entirely

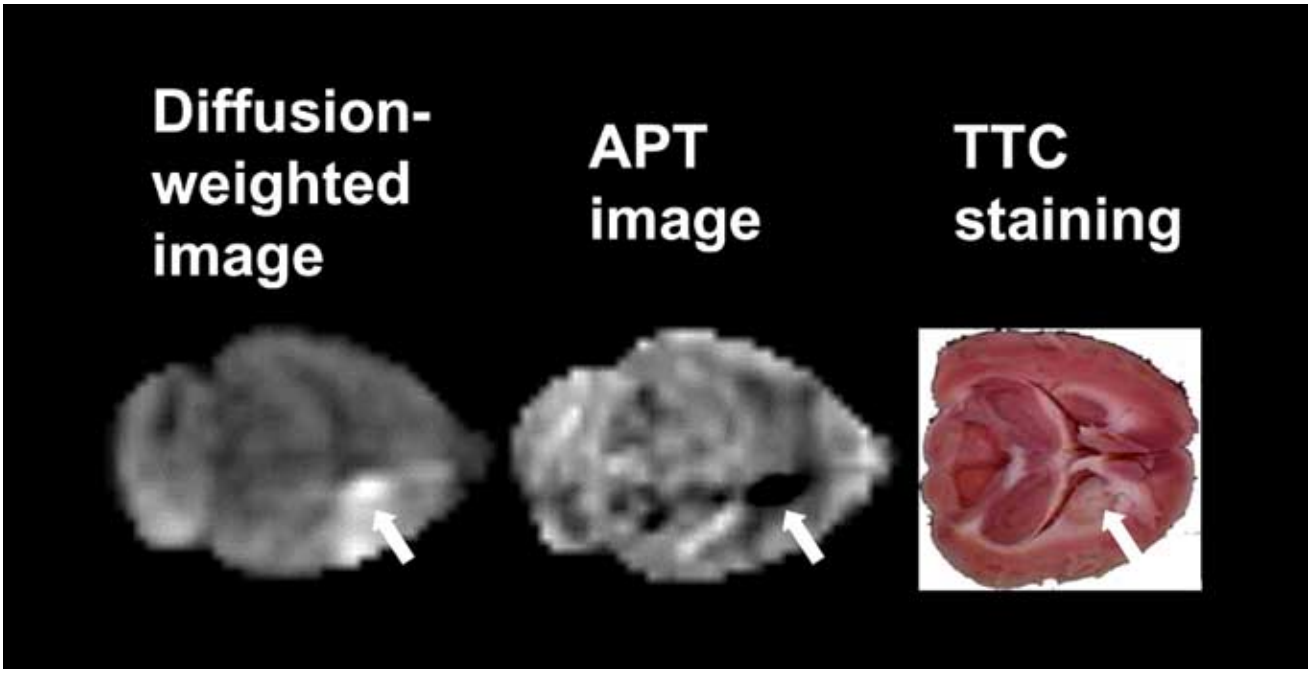

Fig. (11). APT-I imaging of ischemia in rat brain. Note signal dropout at ischemic focus. TTC stains for ischemic regions [178].

intravascular whereas the CT and MR agents tend to leak into the interstitium. US contrast agents are therefore true intravascular agents, simplifying to one compartment the kinetic modeling needed to describe their transit. Another major advantage of US is the capability of real-time imaging, where images may be updated every $1/30^{th}$ of a second [88].

Biomicroscopy

Recently small animal US has been used in phenotyping mice that will be used in the production of knockout strains with cardiovascular anomalies [89]. Doppler US at clinical frequencies (2-10 MHz) is used to detect vascular flow in large vessels, *e.g.*, carotid artery, but is not useful for detecting microvascular changes that occur during tumor angiogenesis. The diameters of the vessels involved in angiogenesis are < 100 μm, necessitating US biomicroscopy. Mouse tumors have been studied with that technique, showing vessels < 20 μm in diameter with a velocity resolution > 1 mm/sec [88]. Probes for biomicroscopy have been developed recently specifically for use in mice, the first applications of which are to study the developing mouse [90].

Contrast-Enhanced US

Contrast-enhanced Doppler US can be used in monitoring anti-angiogenic therapy. Iordanescu *et al.* [91] treated mice engineered to produce prostate tumors *de novo* with vectors producing the Flk1 receptor, an anti-angiogenic protein. They used color Doppler US (15 MHz) and a microbubble-based US contrast agent (6 μm) to study tumor response. Prior to using US, the only way to assess orthotopic abdominal tumors in their models was *via* laparotomy. They demonstrated a decreasing pixel density of the intravascular agent with progression of therapy, indicating response. Sadlowski *et al.* also used contrast-enhanced US to study anti-angiogenic therapy (Sugen) in a rat mammary tumor model, similarly noting a decrease in blood flow with treatment (Fig. **12**). Contrast-enhanced US can be performed with either passive or active targeting [92]. Passive targeting is nonspecific and relies on the diameter of the agent to enable its accumulation at one point in the vasculature or within phagocytic cells. Indications for passive targeting include inflammation, sentinal lymph node detection and the evaluation of tumors of the reticuloendothelial system (liver and spleen). Active (specific) targeting employs adhesion ligands, such as antibodies and peptides, to effect binding in a site-selective fashion. Thrombus is a target of active agents [93]. With active agents, US imaging enters the realm of targeted drug delivery. US bubbles can be fragmented at will to deliver therapeutic agents at their intended site of action, providing a local, relatively nontoxic but concentrated dose (Fig. **13**). For example, Unger *et al.* [94] have produced acoustically active lipospheres containing paclitaxel, a tubulin-stabilizing, antineoplastic agent. Because only one perfluorocarbon-based US contrast agent is approved for clinical use, all experiments involving targeted agents employ small and medium-sized animals.

OPTICAL

Small animal optical imaging is emerging as a versatile tool for therapeutic monitoring of primary tumors, metastases and infection. It can also be used in cell tracking and in imaging gene expression. Small animal optical techniques are essentially adaptations of *in vitro* reporter systems to living animals. Like US, optical imaging provides an essentially instantaneous readout on portable, inexpensive equipment. Several optical techniques, including optical coherence tomography (OCT) [95] and near-infrared (NIR) spectroscopy [96] have made their way into the clinic for specific indications including the interrogation of superficial

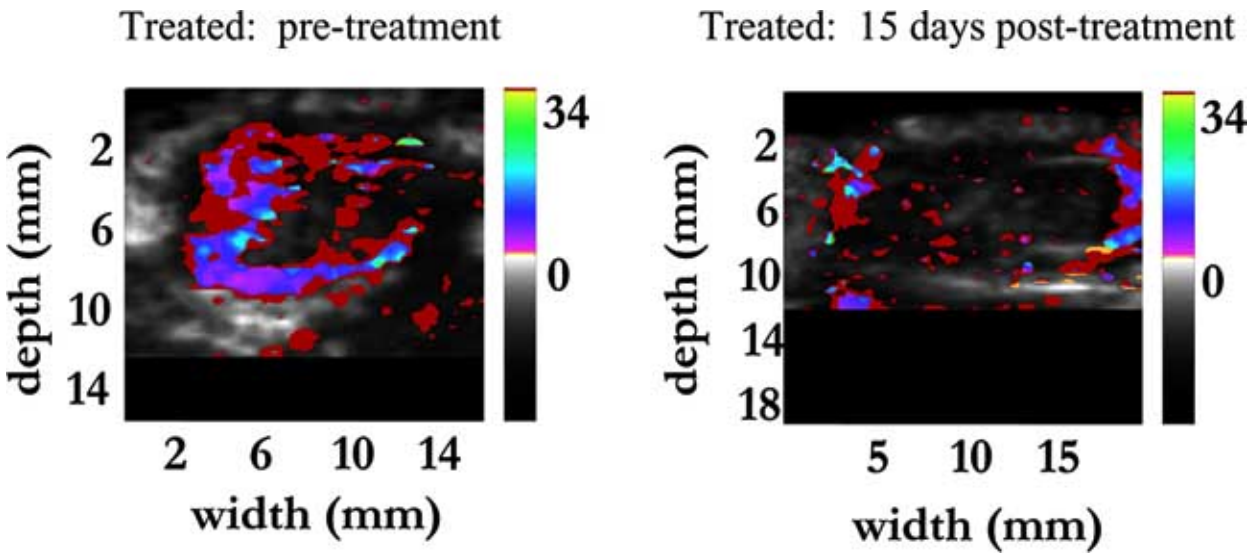

Fig. (12). US imaging of anti-angiogenic therapy. Decreased flow noted after 15 days indicates response [courtesy: Amy Sadlowski, University of California, Davis].

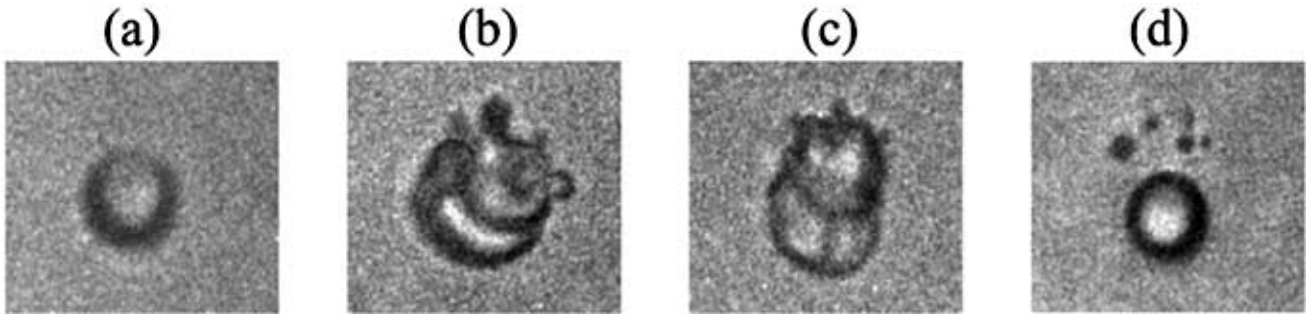

Fig. (13). Fragmentation of an acoustically active liposphere [courtesy: Kathleen Ferrara, University of California, Davis].

structures such as cervix and breast tissue, respectively. NIR has recently been combined with MR in a hybrid system to provide both structural and functional information about breast cancer in the clinic [97].

But the real benefits to drug development lie in the small animal optical imaging techniques of fluorescence imaging, including fluorescence-mediated tomography (FMT), and bioluminescence imaging (BLI). Fluorescence occurs by excitation of the tissue with one wavelength of light and collecting the emitted light, of a longer wavelength, during emission. Charge-coupled-device cameras are used to collect emitted fluorescence. BLI occurs when energy is liberated from a high-energy substrate (luciferin) by a luciferase enzyme upon contact of the two species. The optical techniques are the most sensitive modalities in molecular imaging, with subattomolar ($<10^{-18}$) single-event detection possible *in vitro* for BLI [98]. In practical terms, as few as 100 cells can be detected by BLI in subcutaneous tissues, with 10^6 cells detectable at a depth of 2 cm [20]. Interference from hemoglobin limits depth of penetrance, however the absorbance of hemoglobin decreases significantly at wavelengths > 600 nm, i.e., within the NIR range. Consequently, specific probes for fluorescence imaging are being designed to emit in the NIR [99], and red-shifted mutants of green fluorescent protein (GFP) are sought [100].

Fluorescence Imaging

Fluorescence imaging can be applied in several ways to drug development, including: transfection of experimental tumors [101] or bacteria [102] with a light-emitting protein, *e.g.*, GFP, that can subsequently be followed for response to chemotherapeutics after transplanation to small animal hosts; visualization of transgene expression in selected organs of suitable animal hosts after transfection with, *e.g.*, adenoviral GFP [103] (GFP expression is linked to expression of a gene of interest, as discussed above for the Tf receptor); development of transgenic mice that express GFP in all cells of a particular lineage of interest, *e.g.*, oligodendrocytes [104]; the use of protease-activatable probes [105]; and, receptor-based fluorescent species, *e.g.*, [106]. The response

of an *E. coli*-GFP construct to kanamycin treatment is depicted in Fig. **14** [102]. In analogy to molecular beacons used to isolate oligonucleotides *in vitro* [107], protease-activatable probes emit NIR light upon contact with an enzyme that cleaves them, separating the fluorophor and quencher moieties designed into them. That technique can measure enzyme activity important in certain diseases, such as cathepsins in cancer [108] and atherogenesis, [109]. GFP-based gene expression reporters have been used to validate the radionuclide reporter systems in a dual modality paradigm [80].

BLI

The main advantage of BLI over fluorescence imaging is that it relies on an internal light emitter without competing fluorophors. Consequently there is very little background emission. Administration of an exogenous substrate, luciferin, in reasonably high doses (50 m*M*) suggests that this technique will be restricted to animal use. Probe development is less flexible for BLI than for fluorescence imaging, although many advances in BLI are occurring, including the assay of protein-protein interaction and dual reporter strategies [20]. Uses of BLI to date have been in therapeutic monitoring of tumor treatment and infection as well as in immune cell tracking. Ross *et al.* [110] were able to use BLI to demonstrate the efficacy of 5-fluorocytosine therapy in tumors transfected with the yeast cytosine deaminase (*yCD*) gene.

RADIONUCLIDE

Currently the molecular imaging techniques that employ radiotracers are the most sensitive that are readily translatable to the clinic. For drug development radionuclide imaging has received the most attention, and a professional organization exists promoting industrial-academic collaboration in this enterprise (the Society of Nuclear Imaging in Drug Development, SNIDD). Among the modalities, radionuclide imaging was first that employed functional and molecular imaging because nuclear medicine has always employed molecular probes of varying size and function. The recent marriage of the radionuclide techniques with other modalities, most notably optical imaging, the mapping of the human genome and the development of high-resolution small animal PET and SPECT systems has brought about a surge in new possibilities for using radionuclide techniques in drug development. Almost any drug candidate can be labeled. Key is the ability to determine which candidates are worth the often considerable effort.

The three major drawbacks to the radionuclide techniques are the use of radioactivity, relatively poor spatial and temporal resolution and the expense. The equipment used for radionuclide imaging, particularly PET, is expensive if novel probes (other than FDG) are to be synthesized. The expertise in developing new PET probes is high, but the payoff is also high if knowledge about a specific molecular mechanism is critical to a drug development effort. No other modality has the sensitivity or synthetic flexibility in terms of probe

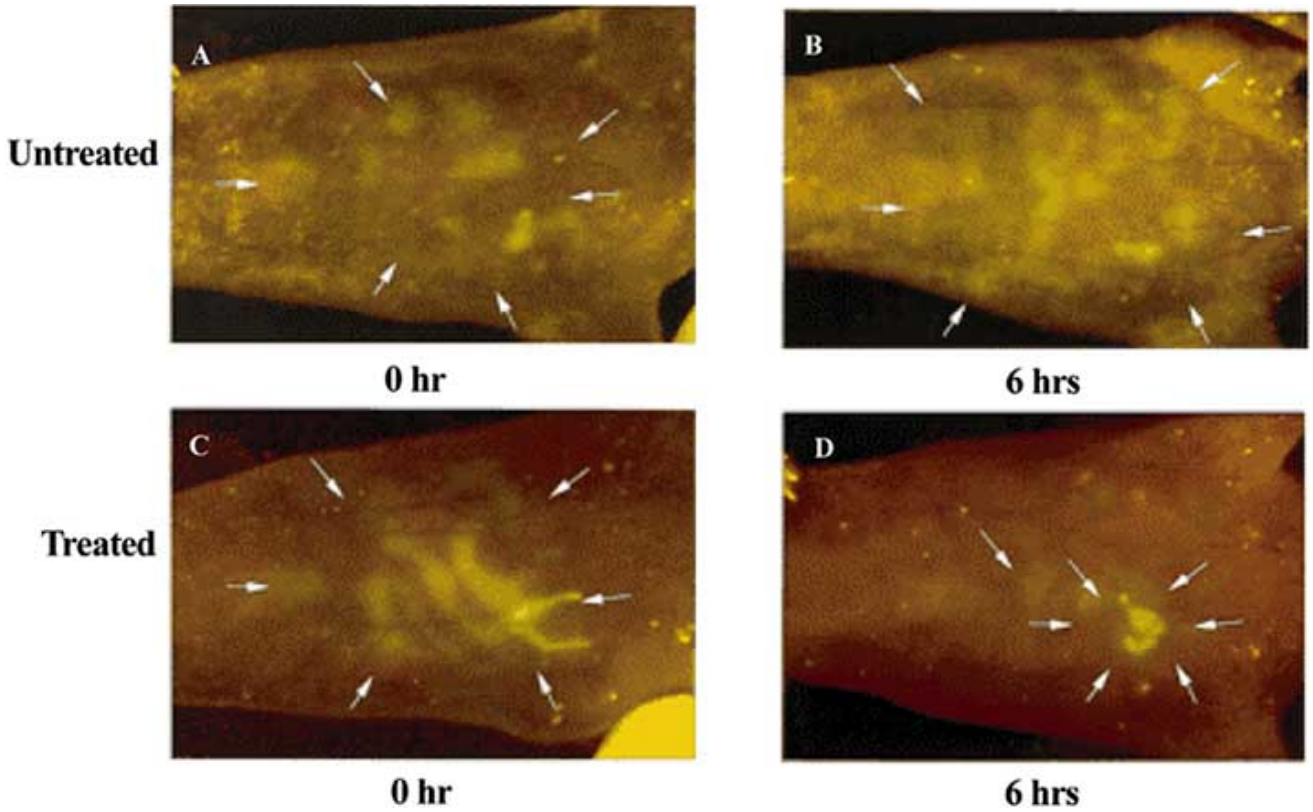

Fig. (14). Fluorescence imaging of antibiotic treatment. The mouse treated with kanamycin 6 hrs after intraperitoneal injection of *E. coli-GFP* survived (C and D) whereas the untreated mouse (A and B) did not [102].

development to interrogate specific cellular pathways and signal transduction cascades, although the optical techniques may prove viable here as well.

Radionuclide imaging can be performed with gamma scintigraphy and planar imaging, SPECT or PET. The resolution and anatomic detail of the device used should be matched to the biological question posed. Planar devices can be perfectly good for assessing BBB permeability of a radiopharmaceutical, for example. When combined with x-ray imaging, planar scintigraphy can be used to good advantage in cell tracking (Fig. **15**).

The relative advantages and disadvantages of SPECT and PET have been debated elsewhere [5], but can be summarized as follows: in general, SPECT enables imaging of biological processes with long half-lives because of the longer physical half-lives of the tracers, has more readily available tracers, employs less expensive equipment and has no theoretical maximum in resolution. PET employs physiologic tracers, i.e., chelation chemistry is not required, the tracers can be identical to the drug candidate to be tested and it lends itself easily to quantification. Commercial packages are now available for tracer kinetic modeling of the more common radiopharmaceuticals. The PET principle relies on certain radionuclides achieving stability by emitting a positron (positive electron) that collides with an electron producing two 511 keV annihilation photons at an angle that approximates 180^{o}. The coincidence of their arrival at opposed detectors marks the recorded event, with various reconstruction algorithms employed to generate a tomographic image. A schematic of a small animal PET ring is shown in Fig. **16** and a small animal PET device, the ATLAS (*A*dvanced *T*echnology *L*aboratory *A*nimal *S*canner), is depicted in Fig. **17**.

Instrumentation

As mentioned above, in principle, the resolution of SPECT imaging with pinhole collimation can be reduced without limit at the cost of sensitivity and/or field-of-view (FOV). That contrasts with PET, in which the positron range and the photon non-colinearity effects intrinsically limit further improvements in resolution. Beekman *et al.* [111] have recently developed a gamma camera that employs micro-pinholes to obtain a spatial resolution of as high as 186 μm using a tracer containing iodine-125. The inherently inefficient mechanical collimation of single photons, however, makes the sensitivity unavoidably low. Long acquisition times and large amounts of injected dose are necessary. The large doses required can violate the assumption of steady state in tracer distribution during the acquisition of a complete set of tomographic projections for some tracers.

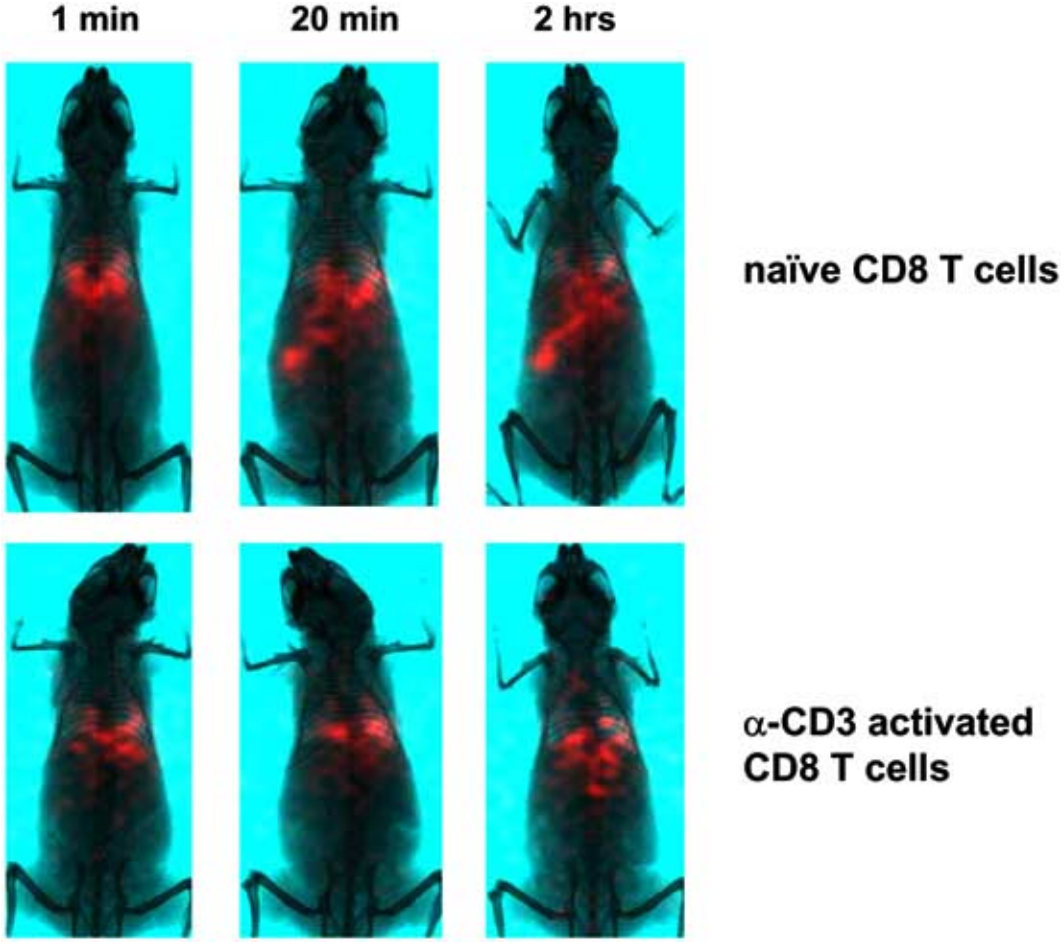

Fig. (15). γ-Imaging of ^{111}In-labeled ex vivo purified CD8 T cells in mice. Activation of T-cells causes increased lung retention and less bowel excretion due to the increased expression of adhesion molecules [courtesy: Mark Williams, University of Virginia].

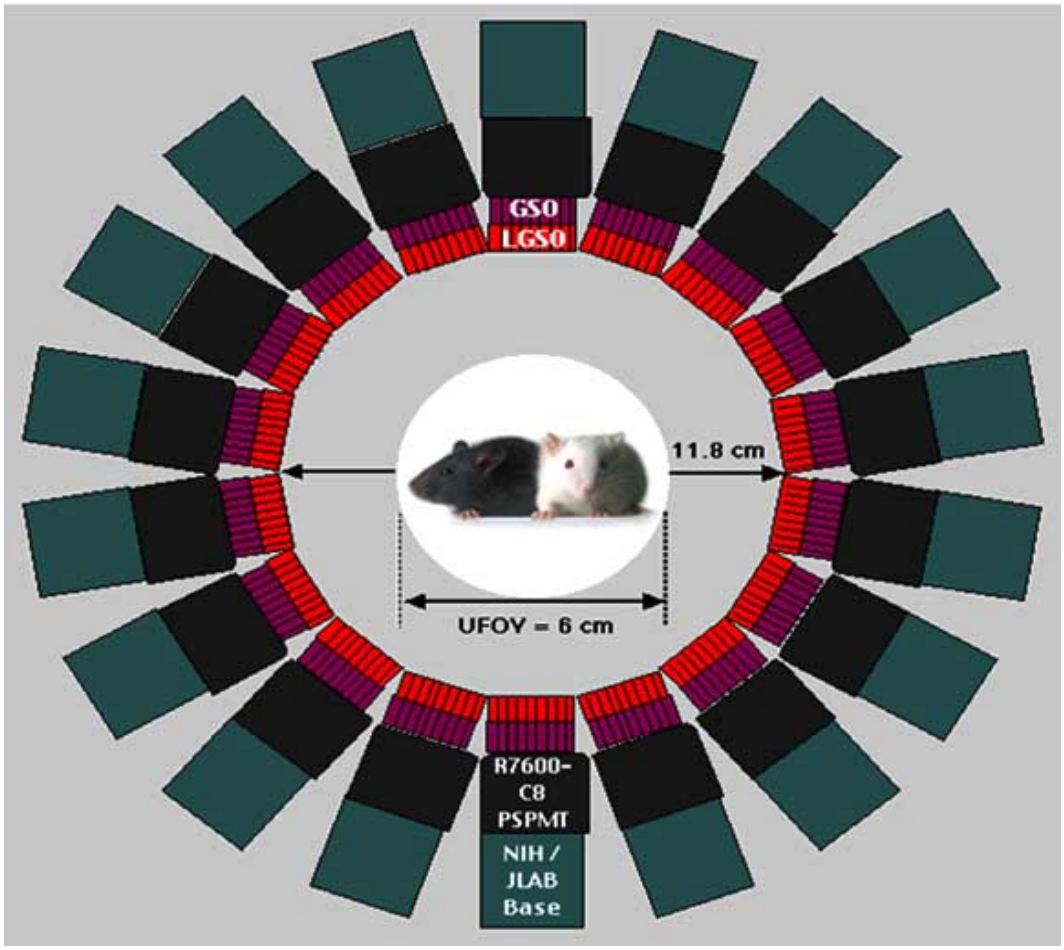

Fig. (16). The NIH ATLAS small animal depth-of-interaction (DOI) PET scanner with LGSO/GSO phoswhich detector modules [courtesy: Michael Green, NIH Clinical Center].

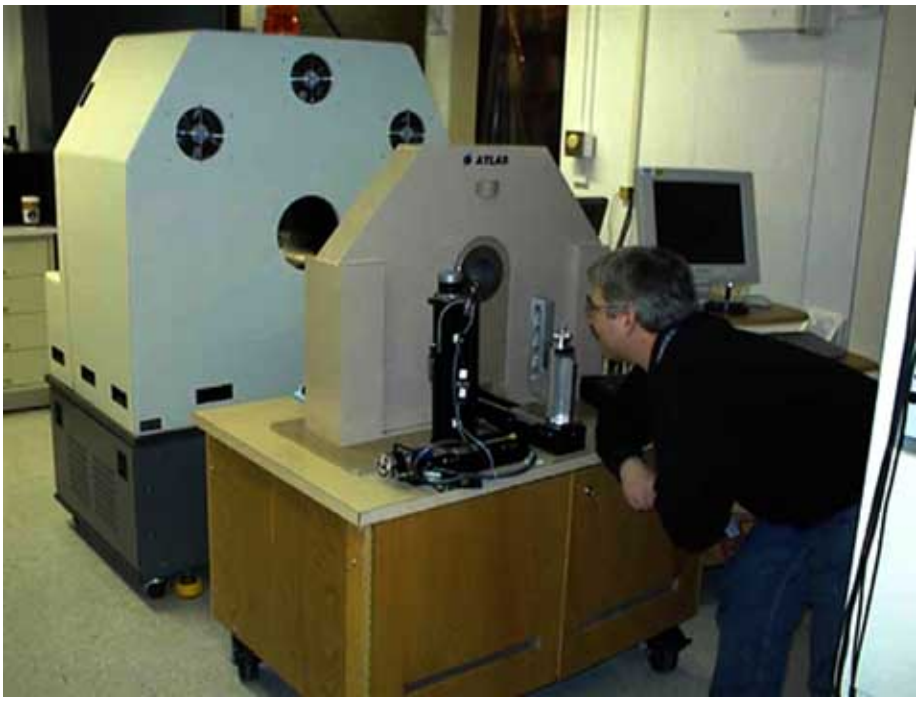

Fig. (17). The NIH ATLAS small animal PET scanner. A microCT device (ImTek, Inc., Knoxville, TN) is present in the background [courtesy: Michael Green, NIH Clinical Center].

The increased amount of injected dose can induce a pharmacologic response and, depending on the specific radioactivity (GBq or mCi/μmol) of the tracer, the radiation absorbed dose received by the animal can cause radiation damage, precluding longitudinal investigations [112]. Limits on injectable dose are also present in small animal PET, as detailed below. Another drawback to SPECT is the inability to perform true dynamic imaging with rotating gamma cameras. Despite those limitations in sensitivity and in dynamic scanning ability, the use of SPECT for small animal imaging will increase since retro-fitting human scanners with specially designed micro pinhole collimators is reasonably easy though suboptimal [113-115] (Fig. **18**). A quantitative study of dopamine transporters in the mouse brain was recently reported using a commercial triple-headed gamma camera equipped with custom-made pinhole collimators [112]. Dedicated animal SPECT systems are under development. LumaGEM A-SPECT, developed by Gamma Medica Inc. (Northridge, CA), is a commercially available dedicated animal pinhole SPECT device. The sensitivity, i.e., percentage of useable detected events, of the camera measured with the 3-mm aperture is 0.07% at 2 cm off-axis, and drops to 0.02% at 4 cm. The spatial resolution of the reconstructed images was on the order of 1.25 mm for images acquired at a radius of rotation (ROR) of 2.4 cm with a 1 mm aperture and even higher for smaller ROR and aperture sizes [116, 117].

In the development of new high-resolution scanners, the goal of PET resolution is 0.5 mm, with submillimeter imaging already demonstrated for at least one system [118]. Table **2** outlines distinguishing features of the small animal PET scanners produced to date. The most widely available dedicated animal PET scanners are those developed by University of California Los Angeles (UCLA) Crump Institute and Concorde MicroSystems Inc. (Knoxville, TN, USA), i.e., the microPET devices. By inheriting the fundamental design of the original UCLA system, Concorde MicroSystems Inc. has commercialized microPET R4 (for rodents) and P4 (for primates) in which some design modifications were made to reduce the overall cost and account for practical manufacturing issues [119, 14]. By increasing the axial FOV, the sensitivity of P4 has been raised to 1.43%, which is about a threefold improvement over the UCLA prototype microPET [119], but resolution

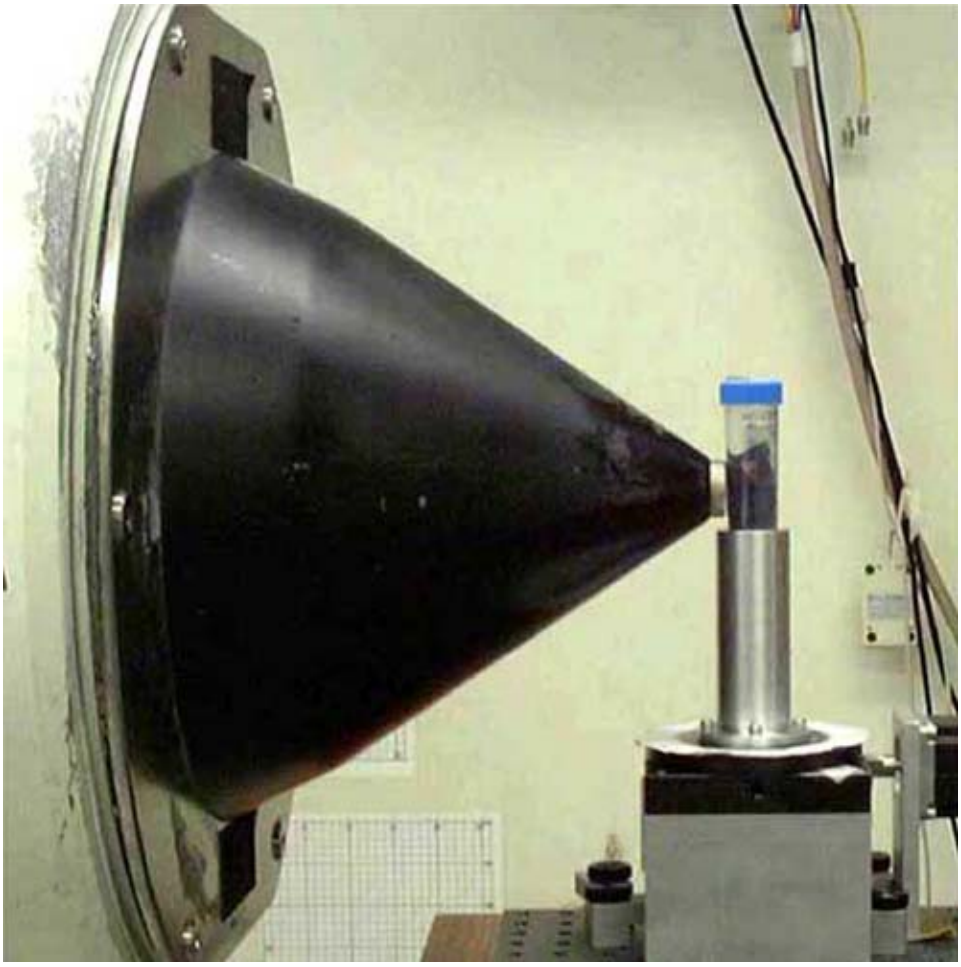

Fig. (18). Pinhole SPECT. System is based on a conventional GE 400 AC LFOV camera and a pinhole collimator with interchangeable pinhole apertures. A small animal can be rotated in front of the pinhole aperture for acquisition of projection data from different angular views [courtesy: Benjamin Tsui, Johns Hopkins University].

remains at or below 2.0 mm. The sensitivity of R4 is known to be nearly 1/3 greater than that of the P4 system. ATLAS is a dual-layer phoswich PET scanner developed at the National Institutes of Health (Bethesda, MD), which has depth of interaction (DOI) capability, enabling increased sensitivity. Spatial resolution at the center of ATLAS is 1.8 mm. Measured absolute sensitivity is 1.8%. Currently many groups are developing dedicated small animal PET scanners in addition to the two detailed above. Reviews of this field have recently appeared [12-14, 120].

Clinical PET has been used in drug development for applications in the CNS, and more recently, oncology. Those are generally quantitative PET studies in which dose finding is undertaken for CNS applications by performing drug candidate receptor occupancy measurements, and the pharmacokinetics and pharmacodynamics of new chemotherapeutic agents are determined. As mentioned above, useful information can be obtained when performing small animal PET on clinical systems, but likely not for animals smaller than rats, i.e., mice. Fig. **19** depicts a series of images from a rat with an RMT breast tumor xenograft. Although the development of a necrotic central core can be appreciated over time, little quantitative information can be extracted from such images. Images on the ATLAS scanner, for example, are of appreciably higher resolution providing the sense that one can be to quantify radiotracer uptake in the small ROIs in rodents.

Receptor-Based Imaging – Challenges

Many reviews of the criteria for developing agents to image low-capacity, high-affinity sites such as receptors, transporters and enzymes have appeared [74, 121-123]. One point to emphasize, however, is that despite the superficial similarity between developing imaging agents and drugs, the two processes are much different. The reason for that is that an imaging agent must clear from regions other than the ROI during the time course of an imaging study *in vivo*, while the biodistribution of a drug is of little consequence, as long as

Table 2. Small Animal PET Scanners

Name	Manufacturer	Ring diameter (cm)	Transverse FOV (cm)	Axial FOV (cm)	Absolute sensitivity (Energy window)	Spatial resolution (mm) (Reconstruction Method)	Ref
microPET	UCLA	17.2	11.25	1.8	0.56% (250~650 keV)	1.8 @ center, 2.0 @ 3 cm (3D FBP)	[166]
microPET-P4	Concorde MicroSystems Inc.	26.0	19.0	7.8	2.25% (250~750 keV)	1.8 @ center, 3.0 @ 4 cm (FORE+2D FBP)	[119]
microPET-R4	Concorde MicroSystems Inc.	14.8	10.0	7.8	~ 3 % (250~800 keV)	1.8 @ center, 3.0 @ 4 cm (FORE+2D FBP)	[119]
Quad-HIDAC	Oxford Positron Systems	17.0	17.0	28.0	1.8% (No energy window)	1.0 @ center (3D OSEM) 0.7 @ center (ROPLE)	[118, 167]
ATLAS	National Institutes of Health	11.8	6.0	2.0	1.8% (250~650 keV)	1.8 @ center, 2.5 @ 3.0 cm (FBP) 1.5 @ center (3D OSEM)	[168, 169]
Tier PET	Univ. of Julich	16-58	4.0	4.0	0.32% (230 keV~)	2.1 @ center (MSRE+2D ML-EM)	[170]
YAPPET	Univ. of Ferrara	10-15	4-10	4.0	1.7 % (50 keV~)	1.8 @ center ~ 1.5 cm (3D Backprojection Filtered)	[171]
VUB-PET	Univ. of Brussels	20.0	11.0	5.2	3.0% (No energy window)	2.6 @ center, 3.8 @ 2.5 cm (FORE+2D FBP)	[172]
MGH PET	Massachusetts General Hospital	12.0	N.A.	0.45	0.08% (150 keV~)	1.2 @ center, 1.7 @ 2.5 cm (2D FBP)	[173]
IndyPET-II	Indiana Univ.	N.A.	23.0	15.0	0.90% (N.A.)	2.5 @ center, 3.5 @ 10 cm (SSR+2D FBP)	[174]
Sherbrooke PET	The Sherbrooke Univ.	31.0	11.8	1.05	0.5% (250~700 keV)	2.1 @ center, 2.4 @ 1 cm (2D FBP)	[175]
MAD-PET	Technischen Univ. Munchen	8.6	6.8	0.2	0.035% (450 keV~)	2.3 @ center, 2.3 @ 1.4 cm (list-mode PWLS)	[176]

FOV: field of view; FBP: filtered backprojection; ML-EM: maximum likelihood expectation maximization; OSEM: ordered subsets expectation maximization; ROPLE: regularized one-pass list-mode expectation maximization; FORE: Fourier rebinning; MSRE: multi slice rebinning; SSR: single slice rebinning; PWLS: penalized weighted least squares.

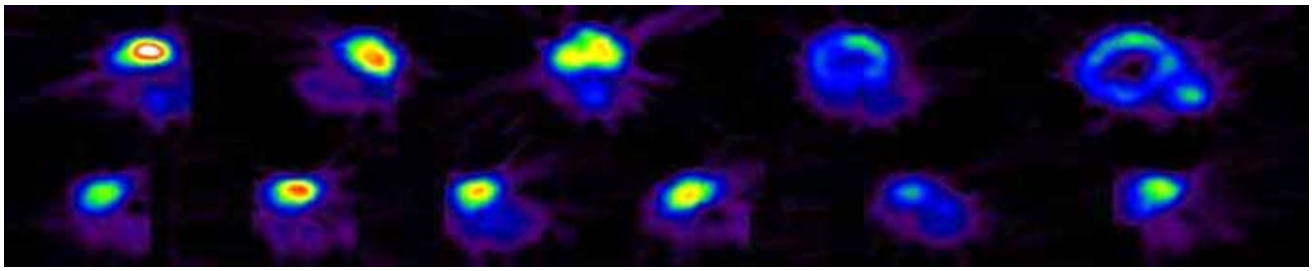

Fig. (19). Breast tumor xenograft. RMT breast tumor is imaged in a rat on a clinical PET device (NeuroECAT). The top row depicts the time course of growth with a necrotic core in last 2 frames. Treated tumor (bottom row) does not expand appreciably [courtesy: Richard Wahl, Johns Hopkins University].

its binding to non-target sites is nontoxic while maintaining activity at the target. That is a great challenge to imaging agent development and a reason for the failure of many.

Receptor-based tracer development has long been the unique domain of radionuclide imaging, mainly because of the high sensitivity of PET (n*M* to p*M*). Receptor-based agents enable either direct (labeled drug) or indirect (receptor occupancy) [124] pharmacokinetic determination of drug candidates. Scaling that process from humans to small animals, even with new high-resolution scanners, is no easy task. Quantitative treatments of that scaling have been undertaken [125], but the main principles will be covered here. First, one must realize that even with dedicated animal scanners the amount of tracer given to an animal must, in general, be comparable to that given to a human. That is because the resolution voxel for the animal is much smaller than that for the human yet the same amount of tracer must be delivered to that voxel for the statistical precision of measurement of activity in that voxel to be the same as for the human. Derivative from this is the issue of the need for very high specific activities for receptor-based radiotracers given to small animals. Since the same amount of radioactivity in the human and animal voxels must be the same, the same degree of mass must be present in the injection. If a PET study involves a radiotracer (MW = 500 Da) at 37 GBq/μmol (1,000 Ci/mmol), for a 70 kg human receiving 370 MBq (10 mCi) of radioactivity, that means a mass load of 7 x 10^{-5} mg/kg. For a mouse, which is 3,500 times less massive than a human, the mass load is 0.25 mg/kg, which may be enough to occupy > 5% of the intended receptor sites, invalidating the tracer principle, particularly for high-affinity (K_d < 1 n*M*) ligands.

Other potential limitations to scaling quantitative PET studies down to mice exist, and include the need for attenuation and scatter correction, correction for partial volume effects and the ability to obtain an arterial input function for full kinetic modeling. The probability that both of the emitted photons travel without scattering to the detectors is

$$P = \exp(-\int_L \mu(x)\,dx) \qquad \text{[eq. 2]}$$

where μ is the 2D function of linear attenuation coefficients, and L is the path corresponding to line of response (LOR) for each detector pair. Assuming a uniform attenuation coefficient of 0.097 cm^{-1} (the attenuation coefficient for water and 511 KeV photons) and length of photon fly path in the body of a rat and mouse to be 5 cm and 3 cm, respectively, approximately 40% and 25% of LOR, respectively, will be lost due to attenuation. However, that does not mean that such a count difference between the deep tissues and the surface of the object will appear in the reconstructed images since the emitted photons from the surface also undergo attenuation through the animal. There is actually a 10-15% difference in counts between the center and peripheral regions when measured using a uniform cylindrical phantom with ~5 cm diameter. As in the clinic, a transmission scan can correct for these errors, particularly for imaging deep structures such as orthotopically-placed tumors. Image co-registration with CT images by retrospective matching or simultaneous acquisition is expected to provide a more reliable way of attenuation correction in small animal PET [126, 127].

Although the spatial resolution of animal PET scanners lies between 1-2 mm, partial volume effects (PVE) will result in errors in the true count estimation due to the small size of the ROI. *A priori* knowledge of the 3D shape and size of the structures determined by image co-registration with CT, MR or ultrasound images is required to correct for PVE [128-131]. Movements of animals or organs are another source of PVE besides the finite resolution of the cameras. Use of devices to restrict the movement of animals, such as a head holder, is required. Electrocardiography and/or respiratory gating can be used to minimize the effects of organ movements [132, 133]. Flexibility in data acquisition, such as listmode acquisition, can also contribute to off-line correction for motion. Correction for PVE can also be incorporated directly into the model used to describe dynamic studies [134-136].

Dynamic PET measures radioactivity over time such that time-activity curves (TACs), delineating tracer uptake and clearance, can be obtained. TACs must be fitted to a mathematical model to describe relevant kinetic parameters of the ligand, i.e., clearance from plasma to tissue (K_1) and vice versa (k_2) and receptor-specific binding (k_3). Tracer kinetic modeling requires the arterial blood input function and correction for the presence of metabolites, which may overlap with the ROI. Radionuclide techniques cannot distinguish between chemically different radioactive species. The input function and blood metabolites are acquired by sampling the arterial or arterialized venous blood in human studies, but that luxury is not readily available in studying

rats and particularly mice [137]. Total blood volume of a rat and mouse is 20 mL and 2.5 mL, respectively, and withdrawal of no more than 10% of total blood is recommended within an hour [14]. Recently, successful application of an advanced blood withdrawal technique to various tracers has been reported in which the arterial blood samples were acquired using catheters placed in the common carotid artery of mice, and metabolites were measured using micro-columns [138, 139]. Automated micro-sampling systems dedicated to small animal imaging have also been developed [140]. Despite those advances in micro-sampling, such direct sampling techniques are technically challenging and difficult to perform repetitively. As the axial FOV of animal PET scanners has been extended and spatial resolution improved, use of image-derived input function from the cardiac chambers or major arteries is gaining use. Various multivariate analysis methods, which have been successfully applied to humans or large animals [141-143] are currently under consideration [144]. Another practical solution for some tracers is use of a population-based, standardized input function, which has been extensively investigated for human PET studies with FDG [145, 146]. Assuming that the shape of the input function is the same across subjects, which is quite reasonable for rodents, except for genetically altered strains, an individual input function can be obtained by calibrating the standardized input function with a small number of blood samples, body weight or body surface area. The reference tissue model for the estimation of binding potential [147, 148] has been used to avoid the use of arterial blood samples in neuroreceptor studies. In that method, the tissue-time activity curve of a region lacking specific binding of the ligand (reference tissue) is used as an indirect input function. Those methods should be, however, carefully evaluated for each radioligand before routine use, since reference regions may not be present for each radioligand.

Applications of Small Animal PET

Studies employing small animal PET to date have not been quantitative in the sense that receptor occupancy, binding potentials (proportional to receptor density) or parametric maps have not been generated. Such quantification will be necessary for small animal PET to see its full potential and replace primates, *e.g.*, in drug development applications. Nevertheless, many important questions can be answered presently. Driving small animal PET has been the desire to image gene expression. That has been reviewed in many recent publications [71, 78, 149-152] but an example germane to drug development is presented here. Using the PET reporter-probe system HSV1-TK/^{124}I-FIAU (FIAU = 2'-fluoro-2'-deoxy-1-beta-D-arabinofuranosyl-5-[^{124}I]iodouracil) Mayer-Kuckuk *et al.* [153] demonstrated that cells exposed to antifolates show a rapid increase in dihydrofolate reductase (DHFR) activity (Fig. **20**). That is an

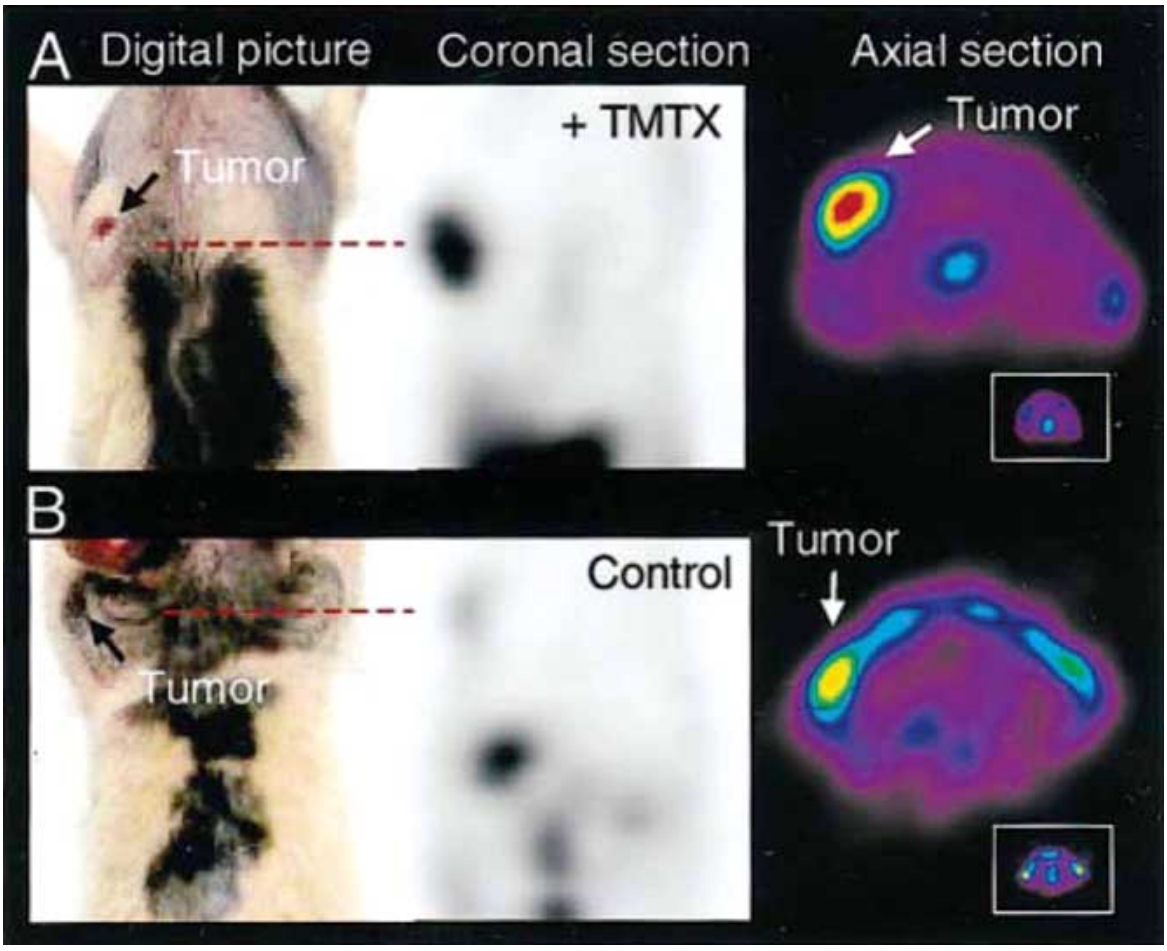

Fig. (20). Imaging Endogenous DHFR Induction. Antifolate treatment (TMTX) upregulates DHFR in panel A. Inset is the heart [153].

example of drug-induced modulation of gene expression and can be used to test the effectiveness of different therapies that act through DHFR.

Haubner *et al.* [154] used small animal PET to assess the effectiveness of ^{18}F-labeled-RGD peptides for imaging alpha(v)beta3 integrin, an adhesion receptor, which will be useful in monitoring vascular therapies. Small animal PET has proved useful for indications in the CNS, including comparing ^{11}C-raclopride uptake in dopamine D_2-receptor deficient mice (PET phenotyping) [155], evaluation of traumatic brain injury [156], brain activation [157], neural repair [158] and in studying a rat model of Huntington's disease [159]. Applications in cardiology include imaging cardiac reporter genes [160] and study of myocardial flow defects in rats with FDG [161]. Cell tracking [162] and protein-protein interactions [21] have been studied with small animal PET. Rodent imaging is beginning to be used in radiopharmaceutical development [163], which will likely be among its most important contributions. Small animal PET will streamline development of radioprobes, which can then be taken into the clinic for continued impact on drug development.

PERSPECTIVE

Rapid scientific advances have characterized molecular imaging and small animal imaging research over the last five years, but substantial challenges remain. From a technical standpoint, the development of small animal imaging devices, particularly for radionuclide applications, has not yet reached the detection limit, i.e., further improvements in sensitivity and resolution are forthcoming, although they will be incremental. Other technical challenges include: timely processing of the vast amounts of data generated by animal studies (one high-resolution mouse study can generate 75 MB of data [36]), particularly if phenotyping or other high-throughput uses of the technology are anticipated; careful validation of the imaging findings with time-tested *in vitro* studies, particularly for gene expression imaging; making the appropriate choices among the many available targets uncovered after sequencing the human genome; and, in the synthesis of suitable probes for those targets. Synthetic chemistry capabilities remain at a premium in imaging research, an area where increased partnership with the pharmaceutical industry could help. In that regard pharma might consider integrating functionality into their drug candidates that will enable them to provide imaging precursors as well as therapeutic agents. Availability of potential imaging agent precursors among the large structural databases of pharma could be pursued more systematically by imaging centers, provided issues regarding intellectual property can be adequately addressed. Many good drugs make poor imaging agents but some poor drugs, shelved by pharma, might be modified into excellent imaging agents.

Sharing intellectual property is not the only non-technical challenge facing molecular imaging research. Gene therapy, one of the target areas of molecular imaging research, is in its infancy and has experienced several setbacks, most recently with the possibly related development of a leukemia-like illness after what appeared to be a success in treating severe combined immunodeficiency disease (SCID) [164]. Also, the specific targets promised by the human genome project, each of which with the potential of an equally specific imaging agent, may not affect many people and therefore may be of limited attractiveness to pharma for therapeutic development. However, just as the Orphan Drug Act of 1983 has been implemented to address that issue, the NCI has implemented several initiatives to enhance the development of imaging agents, including the Development of Clinical Imaging Drugs and Enhancers (DCIDE) program [165].

Deeper understanding of disease processes invariably leads to more specific, less toxic therapy. Patients can now be screened genetically and segregated on that basis before beginning what could be an unnecessary regimen for someone with their genetic composition. Molecular imaging research, initially undertaken in small animals, has been aligned with important goals in therapy, particularly in cancer research, and incorporated into small animal imaging research design has been with a view of translation to the clinic. Initial clinical applications of this body of work will likely involve cell tracking, using radionuclide techniques, but the long-term applications will extend to providing imaging phenotypes for patients, rendering large-scale screening processes obsolete. Drug development will benefit not only through cost savings at many pre-clinical and clinical steps, but also by improving the efficiency of research programs in pharma, which will be free to tackle more feasible and relevant targets.

ACKNOWLEDGEMENTS

We thank Benjamin Tsui and Michael Green for helpful discussions. Support was provided by R24CA92871.

Portions of this manuscript have appeared in the Journal of Cellular Biochemistry (2002; Suppl. 39, pp. 211-220).

REFERENCES

References 179-181 are related articles recently published in Current Pharmaceutical Design.

[1] Gregory SG, Sekhon M, Schein J, Zhao S, Osoegawa K, Scott CE, *et al*. A physical map of the mouse genome. Nature 2002; 418(6899): 743-50.

[2] Gupta N, Price PM, Aboagye EO. PET for *in vivo* pharmacokinetic and pharmacodynamic measurements. Eur J Cancer 2002; 38(16): 2094.

[3] Hietala J. Ligand-receptor interactions as studied by PET: implications for drug development. Ann Med 1999; 31(6): 438-43.

[4] Rubin RH, Fischman AJ. Positron emission tomography in drug development. Q J Nucl Med 1997; 41(2): 171-5.

[5] Gibson RE, Burns HD, Eckelman WC. The potential uses of radiopharmaceuticals in the pharmaceutical industry. In: Burns HD, Gibson R, Dannals R, Siegl P, editors. Nuclear Imaging in Drug Discovery, Development, and Approval. Boston: Birkhauser; 1993. p. 321-331.

[6] Paans AM, Vaalburg W. Positron emission tomography in drug development and drug evaluation. Curr Pharm Des 2000; 6(16): 1583-91.

[7] Vaalburg W, Hendrikse NH, de Vries EF. Drug development, radiolabelled drugs and PET. Ann Med 1999; 31(6): 432-7.

[8] Fowler JS, Volkow ND, Wang GJ, Ding YS, Dewey SL. PET and drug research and development. J Nucl Med 1999; 40(7): 1154-63.

[9] Aboagye EO, Price PM, Jones T. *In vivo* pharmacokinetics and pharmacodynamics in drug development using positron-emission tomography. Drug Discov Today 2001; 6(6): 293-302.

[10] Brady F, Luthra SK, Brown GD, Osman S, Aboagye E, Saleem A, *et al*. Radiolabelled tracers and anticancer drugs for assessment of therapeutic efficacy using PET. Curr Pharm Des 2001; 7(18): 1863-92.
[11] Eckelman WC, Waterhouse R, Frank R. Nuclear imaging and biomarkers in drug development using approved radiopharmaceuticals. J Clin Pharmacol 2001; Suppl: 4S-6S.
[12] Hume SP, Myers R. Dedicated small animal scanners: a new tool for drug development? Curr Pharm Des 2002; 8(16): 1497-511.
[13] Myers R. The biological application of small animal PET imaging. Nucl Med Biol 2001; 28(5): 585-93.
[14] Chatziioannou AF. Molecular imaging of small animals with dedicated PET tomographs. Eur J Nucl Med Mol Imaging 2002; 29(1): 98-114.
[15] Kreider BL. Proteomics: defining protein function in the post genomics era. In: Doherty AM, editor. Annual Reports in Medicinal Chemistry. New York: Academic 2001; p. 227-235.
[16] MacBeath G, Schreiber SL. Printing proteins as microarrays for high-throughput function determination. Science 2000; 289(5485): 1760-3.
[17] Pomper MG, Musachio JL, Scheffel U, Macdonald JE, McCarthy DJ, Reif DW, *et al.* Radiolabeled neuronal nitric oxide synthase inhibitors: synthesis, *in vivo* evaluation, and primate PET studies. J Nucl Med 2000; 41(8): 1417-25.
[18] Smith GP, Petrenko VA. Phage Display. Chem Rev 1997; 97(2): 391-410.
[19] Nixon AE. Phage display as a tool for protease ligand discovery. Curr Pharm Biotechnol 2002; 3(1): 1-12.
[20] Contag CH, Ross BD. It's not just about anatomy: *In vivo* bioluminescence imaging as an eyepiece into biology. J Magn Reson Imaging 2002; 16(4): 378-87.
[21] Luker GD, Sharma V, Pica CM, Dahlheimer JL, Li W, Ochesky J, *et al*. Noninvasive imaging of protein-protein interactions in living animals. Proc Natl Acad Sci USA 2002; 99(10): 6961-6.
[22] Druker BJ, Tamura S, Buchdunger E, Ohno S, Segal GM, Fanning S, *et al*. Effects of a selective inhibitor of the Abl tyrosine kinase on the growth of Bcr-Abl positive cells. Nat Med 1996; 2(5): 561-6.
[23] Montelione GT. Structural genomics: an approach to the protein folding problem. Proc Natl Acad Sci USA 2001; 98(24): 13488-9.
[24] Grunder G, Yokoi F, Offord SJ, Ravert HT, Dannals RF, Salzmann JK, *et al*. Time course of 5-HT2A receptor occupancy in the human brain after a single oral dose of the putative antipsychotic drug MDL 100,907 measured by positron emission tomography. Neuropsychopharmacology 1997; 17(3): 175-85.
[25] Padhani AR, Ollivier L. The RECIST (Response Evaluation Criteria in Solid Tumors) criteria: implications for diagnostic radiologists. Br J Radiol 2001; 74(887): 983-6.
[26] Hoekstra CJ, Hoekstra OS, Stroobants SG, Vansteenkiste J, Nuyts J, Smit EF, *et al*. Methods to monitor response to chemotherapy in non-small cell lung cancer with 18F-FDG PET. J Nucl Med 2002; 43(10): 1304-9.
[27] Dittmann H, Dohmen BM, Kehlbach R, Bartusek G, Pritzkow M, Sarbia M, *et al*. Early changes in [(18)F]FLT uptake after chemotherapy: an experimental study. Eur J Nucl Med Mol Imaging 2002; 29(11): 1462-9.
[28] Bluemke DA, Stillman AE, Bis KG, Grist TM, Baum RA, D'Agostino R, *et al*. Carotid MR angiography: phase II study of safety and efficacy for MS-325. Radiology 2001; 219(1): 114-22.
[29] Schellens JH, Malingre MM, Kruijtzer CM, Bardelmeijer HA, van Tellingen O, Schinkel AH, *et al*. Modulation of oral bioavailability of anticancer drugs: from mouse to man. Eur J Pharm Sci 2000; 12(2): 103-10.
[30] Perez-Soler R, Kemp B, Wu QP, Mao L, Gomez J, Zeleniuch-Jacquotte A, *et al*. Response and determinants of sensitivity to paclitaxel in human non-small cell lung cancer tumors heterotransplanted in nude mice. Clin Cancer Res 2000; 6(12): 4932-8.
[31] Flecknell PA. Anaesthesia of animals for biomedical research. Br J Anaesth 1993; 71(6): 885-94.
[32] Arras M, Autenried P, Rettich A, Spaeni D, Rulicke T. Optimization of intraperitoneal injection anesthesia in mice: drugs, dosages, adverse effects, and anesthesia depth. Comp Med 2001; 51(5): 443-56.
[33] Balaban RS, Hampshire VA. Challenges in small animal noninvasive imaging. Ilar J 2001; 42(3): 248-62.
[34] Sessions A, Eichel L, Kassahun M, Messing EM, Schwarz E, Wood RW. Continuous bladder infusion methods for studying voiding function in the ambulatory mouse. Urology 2002; 60(4): 707.
[35] Brau AC, Wheeler CT, Hedlund LW, Johnson GA. Fiber-optic stethoscope: a cardiac monitoring and gating system for magnetic resonance microscopy. Magn Reson Med 2002; 47(2): 314-21.
[36] Weissleder R. Scaling down imaging: molecular mapping of cancer in mice. Nat Rev Cancer 2002; 2(1): 11-8.
[37] Paulus MJ, Gleason SS, Easterly ME, Foltz CJ. A review of high-resolution X-ray computed tomography and other imaging modalities for small animal research. Lab Anim (NY) 2001; 30(3): 36-45.
[38] Kennel SJ, Davis IA, Branning J, Pan H, Kabalka GW, Paulus MJ. High resolution computed tomography and MRI for monitoring lung tumor growth in mice undergoing radioimmunotherapy: correlation with histology. Med Phys 2000; 27(5): 1101-7.
[39] Andersson N, Lindberg MK, Ohlsson C, Andersson K, Ryberg B. Repeated *in vivo* determinations of bone mineral density during parathyroid hormone treatment in ovariectomized mice. J Endocrinol 2001; 170(3): 529-37.
[40] Street J, Bao M, deGuzman L, Bunting S, Peale FV Jr, Ferrara N, *et al*. Vascular endothelial growth factor stimulates bone repair by promoting angiogenesis and bone turnover. Proc Natl Acad Sci USA 2002; 99(15): 9656-61.
[41] Bentley MD, Ortiz MC, Ritman EL, Romero JC. The use of microcomputed tomography to study microvasculature in small rodents. Am J Physiol Regul Integr Comp Physiol 2002; 282(5): R1267-79.
[42] Torchilin VP, Frank-Kamenetsky MD, Wolf GL. CT visualization of blood pool in rats by using long-circulating, iodine-containing micelles. Acad Radiol 1999; 6(1): 61-5.
[43] Leike JU, Sachse A, Rupp K. Characterization of continuously extruded iopromide-carrying liposomes for computed tomography blood-pool imaging. Invest Radiol 2001; 36(6): 303-8.
[44] Charnsangavej C, Kan Z, Tang Y, Silvana F, D. H, Lee RT, *et al*. High-resolution functional CT in quantification of antiangiogenic therapy: a preliminary study in animal model. In: HiRes 2001; Washington, DC. 2001; p. 102-104.
[45] Gillies RJ, Raghunand N, Karczmar GS, Bhujwalla ZM. MRI of the tumor microenvironment. J Magn Reson Imaging 2002; 16(4): 430-50.
[46] Stohrer M, Boucher Y, Stangassinger M, Jain RK. Oncotic pressure in solid tumors is elevated. Cancer Res 2000; 60(15): 4251-5.
[47] Cuellar DC, Rhee J, Kyprianou N. Alpha1-adrenoceptor antagonists radiosensitize prostate cancer cells *via* apoptosis induction. Anticancer Res 2002; 22(3): 1673-9.
[48] Huang SM, Li J, Armstrong EA, Harari PM. Modulation of radiation response and tumor-induced angiogenesis after epidermal growth factor receptor inhibition by ZD1839 (Iressa). Cancer Res 2002; 62(15): 4300-6.
[49] Wise RG, Rogers R, Painter D, Bantick S, Ploghaus A, Williams P, *et al*. Combining fMRI with a pharmacokinetic model to determine which brain areas activated by painful stimulation are specifically modulated by remifentanil. Neuroimage 2002; 16(4): 999-1014.
[50] Tracey I. Prospects for human pharmacological functional magnetic resonance imaging (phMRI). J Clin Pharmacol 2001; Suppl: 21S-28S.
[51] Muruganandham M, Kasiviswanathan A, Jagannathan NR, Raghunathan P, Jain PC, Jain V. Diltiazem enhances tumor blood flow: MRI study in a murine tumor. Int J Radiat Oncol Biol Phys 1999; 43(2): 413-21.
[52] Shaharabany M, Abramovitch R, Kushnir T, Tsarfaty G, Ravid-Megido M, Horev J, *et al*. *In vivo* molecular imaging of met tyrosine kinase growth factor receptor activity in normal organs and breast tumors. Cancer Res 2001; 61(12): 4873-8.
[53] Morotti A, Mila S, Accornero P, Tagliabue E, Ponzetto C. K252a inhibits the oncogenic properties of Met, the HGF receptor. Oncogene 2002; 21(32): 4885-93.
[54] Bhujwalla ZM, Artemov D, Ballesteros P, Cerdan S, Gillies RJ, Solaiyappan M. Combined vascular and extracellular pH imaging of solid tumors. NMR Biomed 2002; 15(2): 114-9.
[55] Van Zijl PC, Barker PB. Magnetic resonance spectroscopy and spectroscopic imaging for the study of brain metabolism. Ann N Y Acad Sci 1997; 820: 75-96.

[56] Aboagye EO, Artemov D, Senter PD, Bhujwalla ZM. Intratumoral conversion of 5-fluorocytosine to 5-fluorouracil by monoclonal antibody-cytosine deaminase conjugates: noninvasive detection of prodrug activation by magnetic resonance spectroscopy and spectroscopic imaging. Cancer Res 1998; 58(18): 4075-8.

[57] Van Zijl PC, Davis D, Eleff SM, Moonen CT, Parker RJ, Strong JM. Determination of cerebral glucose transport and metabolic kinetics by dynamic MR spectroscopy. Am J Physiol 1997; 273(6 Pt 1): E1216-27.

[58] Artemov D, Solaiyappan M, Bhujwalla ZM. Magnetic resonance pharmacoangiography to detect and predict chemotherapy delivery to solid tumors. Cancer Res 2001; 61(7): 3039-44.

[59] Saeed M, Wendland MF, Watzinger N, Akbari H, Higgins CB. MR contrast media for myocardial viability, microvascular integrity and perfusion. Eur J Radiol 2000; 34(3): 179-95.

[60] Calamante F, Gadian DG, Connelly A. Quantification of perfusion using bolus tracking magnetic resonance imaging in stroke: assumptions, limitations, and potential implications for clinical use. Stroke 2002; 33(4): 1146-51.

[61] Beckmann N, Hof RP, Rudin M. The role of magnetic resonance imaging and spectroscopy in transplantation: from animal models to man. NMR Biomed 2000; 13(6): 329-48.

[62] Padhani AR. Dynamic contrast-enhanced MRI in clinical oncology: Current status and future directions. J Magn Reson Imaging 2002; 16(4): 407-22.

[63] Salmeron BJ, Stein EA. Pharmacological applications of magnetic resonance imaging. Psychopharmacol Bull 2002; 36(1): 102-29.

[64] Detre JA, Zhang W, Roberts DA, Silva AC, Williams DS, Grandis DJ, *et al*. Tissue specific perfusion imaging using arterial spin labeling. NMR Biomed 1994; 7(1-2): 75-82.

[65] Larsson HB, Stubgaard M, Frederiksen JL, Jensen M, Henriksen O, Paulson OB. Quantitation of blood-brain barrier defect by magnetic resonance imaging and gadolinium-DTPA in patients with multiple sclerosis and brain tumors. Magn Reson Med 1990; 16(1): 117-31.

[66] Tofts PS. Modeling tracer kinetics in dynamic Gd-DTPA MR imaging. J Magn Reson Imaging 1997; 7(1): 91-101.

[67] Bhujwalla ZM, Artemov D, Natarajan K, Ackerstaff E, Solaiyappan M. Vascular differences detected by MRI for metastatic versus nonmetastatic breast and prostate cancer xenografts. Neoplasia 2001; 3(2): 143-53.

[68] Su MY, Taylor JA, Villarreal LP, Nalcioglu O. Prediction of gene therapy-induced tumor size changes by the vascularity changes measured using dynamic contrast-enhanced MRI. Magn Reson Imaging 2000; 18(3): 311-7.

[69] Pomper MG, Port JD. New techniques in MR imaging of brain tumors. Magn Reson Imaging Clin N Am 2000; 8(4): 691-713.

[70] Chenevert TL, Stegman LD, Taylor JM, Robertson PL, Greenberg HS, Rehemtulla A, *et al*. Diffusion magnetic resonance imaging: an early surrogate marker of therapeutic efficacy in brain tumors. J Natl Cancer Inst 2000; 92(24): 2029-36.

[71] Louie AY, Huber MM, Ahrens ET, Rothbacher U, Moats R, Jacobs RE, *et al*. *In vivo* visualization of gene expression using magnetic resonance imaging. Nat Biotechnol 2000; 18(3): 321-5.

[72] Li WH, Parigi G, Fragai M, Luchinat C, Meade TJ. Mechanistic studies of a calcium-dependent MRI contrast agent. Inorg Chem 2002; 41(15): 4018-24.

[73] Josephson L, Tung CH, Moore A, Weissleder R. High-efficiency intracellular magnetic labeling with novel superparamagnetic-Tat peptide conjugates. Bioconjug Chem 1999; 10(2): 186-91.

[74] Eckelman WC, Frank JA, Brechbiel M. Theory and practice of imaging saturable binding sites. Invest Radiol 2002; 37(3): 101-6.

[75] Schoepf U, Marecos EM, Melder RJ, Jain RK, Weissleder R. Intracellular magnetic labeling of lymphocytes for *in vivo* trafficking studies. Biotechniques 1998; 24(4): 642-6, 648-51.

[76] Bulte JW, Douglas T, Witwer B, Zhang SC, Lewis BK, van Gelderen P, *et al*. Monitoring stem cell therapy *in vivo* using magnetodendrimers as a new class of cellular MR contrast agents. Acad Radiol 2002; 9(Suppl 2): S332-5.

[77] Goffeney N, Bulte JW, Duyn J, Bryant LH Jr, van Zijl PC. Sensitive NMR detection of cationic-polymer-based gene delivery systems using saturation transfer *via* proton exchange. J Am Chem Soc 2001; 123(35): 8628-9.

[78] Weissleder R, Moore A, Mahmood U, Bhorade R, Benveniste H, Chiocca EA, *et al*. *In vivo* magnetic resonance imaging of transgene expression. Nat Med 2000; 6(3): 351-5.

[79] Moore A, Josephson L, Bhorade RM, Basilion JP, Weissleder R. Human transferrin receptor gene as a marker gene for MR imaging. Radiology 2001; 221(1): 244-50.

[80] Jacobs A, Dubrovin M, Hewett J, Sena-Esteves M, Tan CW, Slack M, *et al*. Functional coexpression of HSV-1 thymidine kinase and green fluorescent protein: implications for noninvasive imaging of transgene expression. Neoplasia 1999; 1(2): 154-61.

[81] Lewin M, Carlesso N, Tung CH, Tang XW, Cory D, Scadden DT, *et al*. Tat peptide-derivatized magnetic nanoparticles allow *in vivo* tracking and recovery of progenitor cells. Nat Biotechnol 2000; 18(4): 410-4.

[82] Modo M, Cash D, Mellodew K, Williams S, Fraser S, Meade T, *et al*. Tracking transplanted stem cell migration using bifunctional, contrast agent-enhanced, magnetic resonance imaging. Neuroimage 2002; 17(2): 803.

[83] Bulte JW, Douglas T, Witwer B, Zhang SC, Strable E, Lewis BK, *et al*. Magnetodendrimers allow endosomal magnetic labeling and *in vivo* tracking of stem cells. Nat Biotechnol 2001; 19(12): 1141-7.

[84] Weissleder R, Cheng HC, Bogdanova A, Bogdanov A, Jr. Magnetically labeled cells can be detected by MR imaging. J Magn Reson Imaging 1997; 7(1): 258-63.

[85] Yeh TC, Zhang W, Ildstad ST, Ho C. *In vivo* dynamic MRI tracking of rat T-cells labeled with superparamagnetic iron-oxide particles. Magn Reson Med 1995; 33(2): 200-8.

[86] Bulte JW, Zhang S, van Gelderen P, Herynek V, Jordan EK, Duncan ID, *et al*. Neurotransplantation of magnetically labeled oligodendrocyte progenitors: magnetic resonance tracking of cell migration and myelination. Proc Natl Acad Sci USA 1999; 96(26): 15256-61.

[87] Foster FS, Burns PN, Simpson DH, Wilson SR, Christopher DA, Goertz DE. Ultrasound for the visualization and quantification of tumor microcirculation. Cancer Metastasis Rev 2000; 19(1-2): 131-8.

[88] Ferrara KW, Merritt CR, Burns PN, Foster FS, Mattrey RF, Wickline SA. Evaluation of tumor angiogenesis with US: imaging, Doppler, and contrast agents. Acad Radiol 2000; 7(10): 824-39.

[89] Guo X, Kono Y, Mattrey R, Kassab GS. Morphometry and strain distribution of the C57BL/6 mouse aorta. Am J Physiol Heart Circ Physiol 2002; 283(5): H1829-37.

[90] Foster FS, Zhang MY, Zhou YQ, Liu G, Mehi J, Cherin E, *et al*. A new ultrasound instrument for *in vivo* microimaging of mice. Ultrasound Med Biol 2002; 28(9): 1165-1172.

[91] Iordanescu I, Becker C, Zetter B, Dunning P, Taylor GA. Tumor vascularity: evaluation in a murine model with contrast-enhanced color Doppler US effect of angiogenesis inhibitors. Radiology 2002; 222(2): 460-7.

[92] Dayton PA, Ferrara KW. Targeted imaging using ultrasound. J Magn Reson Imaging 2002; 16(4): 362-77.

[93] Schumann PA, Christiansen JP, Quigley RM, McCreery TP, Sweitzer RH, Unger EC, *et al*. Targeted-Microbubble Binding Selectively to GPIIb IIIa Receptors of Platelet Thrombi. Invest Radiol 2002; 37(11): 587-593.

[94] Unger EC, McCreery TP, Sweitzer RH, Caldwell VE, Wu Y. Acoustically active lipospheres containing paclitaxel: a new therapeutic ultrasound contrast agent. Invest Radiol 1998; 33(12): 886-92.

[95] Fujimoto JG, Pitris C, Boppart SA, Brezinski ME. Optical coherence tomography: an emerging technology for biomedical imaging and optical biopsy. Neoplasia 2000; 2(1-2): 9-25.

[96] Shah N, Cerussi A, Eker C, Espinoza J, Butler J, Fishkin J, *et al*. Noninvasive functional optical spectroscopy of human breast tissue. Proc Natl Acad Sci USA 2001; 98(8): 4420-5.

[97] Ntziachristos V, Yodh AG, Schnall MD, Chance B. MRI-Guided Diffuse Optical Spectroscopy of Malignant and Benign Breast Lesions. Neoplasia 2002; 4(4): 347-54.

[98] Benaron DA, Contag PR, Contag CH. Imaging brain structure and function, infection and gene expression in the body using light. Philos Trans R Soc Lond B Biol Sci 1997; 352(1354): 755-61.

[99] Lin Y, Weissleder R, Tung CH. Novel near-infrared cyanine fluorochromes: synthesis, properties, and bioconjugation. Bioconjug Chem 2002; 13(3): 605-10.

[100] Matz MV, Lukyanov KA, Lukyanov SA. Family of the green fluorescent protein: Journey to the end of the rainbow. Bioessays 2002; 24(10): 953-9.

[101] Yang M, Baranov E, Wang JW, Jiang P, Wang X, Sun FX, *et al*. Direct external imaging of nascent cancer, tumor progression,

angiogenesis, and metastasis on internal organs in the fluorescent orthotopic model. Proc Natl Acad Sci USA 2002; 99(6): 3824-9.

[102] Zhao M, Yang M, Baranov E, Wang X, Penman S, Moossa AR, *et al*. Spatial-temporal imaging of bacterial infection and antibiotic response in intact animals. Proc Natl Acad Sci USA 2001; 98(17): 9814-8.

[103] Yang M, Baranov E, Moossa AR, Penman S, Hoffman RM. Visualizing gene expression by whole-body fluorescence imaging. Proc Natl Acad Sci USA 2000; 97(22): 12278-82.

[104] Yuan X, Chittajallu R, Belachew S, Anderson S, McBain CJ, Gallo V. Expression of the green fluorescent protein in the oligodendrocyte lineage: A transgenic mouse for developmental and physiological studies. J Neurosci Res 2002; 70(4): 529-45.

[105] Tung CH, Mahmood U, Bredow S, Weissleder R. *In vivo* imaging of proteolytic enzyme activity using a novel molecular reporter. Cancer Res 2000; 60(17): 4953-8.

[106] Wong AC, Shetreat ME, Clarke JO, Rayport S. D1- and D2-like dopamine receptors are co-localized on the presynaptic varicosities of striatal and nucleus accumbens neurons *in vitro*. Neuroscience 1999; 89(1): 221-33.

[107] Marras SA, Kramer FR, Tyagi S. Efficiencies of fluorescence resonance energy transfer and contact-mediated quenching in oligonucleotide probes. Nucleic Acids Res 2002; 30(21): E122-2.

[108] Mahmood U, Tung CH, Bogdanov A Jr, Weissleder R. Near-infrared optical imaging of protease activity for tumor detection. Radiology 1999; 213(3): 866-70.

[109] Chen J, Tung CH, Mahmood U, Ntziachristos V, Gyurko R, Fishman MC, *et al*. *In vivo* imaging of proteolytic activity in atherosclerosis. Circulation 2002; 105(23): 2766-71.

[110] Ross BD, Chenevert TL, Rehemtulla A. Magnetic resonance imaging in cancer research. Eur J Cancer 2002; 38(16): 2147.

[111] Beekman FJ, McElroy DP, Berger F, Gambhir SS, Hoffman EJ, Cherry SR. Towards *in vivo* nuclear microscopy: iodine-125 imaging in mice using micro-pinholes. Eur J Nucl Med Mol Imaging 2002; 29(7): 933-8.

[112] Acton PD, Kung MP, Hou C, Plossl K, Keeney C, Kung HF. Ultra-high resolution single photon emission tomography imaging of the mouse striatum. Eur J Nucl Med Mol Imaging 2002; 29(3): 446.

[113] Jaszczak RJ, Li J, Wang H, Zalutsky MR, Coleman RE. Pinhole collimation for ultra high resolution small field of view SPECT. Phys Med Biol 1994; 39: 425-437.

[114] Ishizu K, Mukai T, Yonekura Y, Pagani M, Fujita T, Magata Y, *et al*. Ultra-high resolution SPECT system using four pinhole collimators for small animal studies. J Nucl Med 1995; 36(12): 2282-7.

[115] Weber DA, Ivanovic M. Pinhole SPECT: ultra-high resolution imaging for small animal studies. J Nucl Med 1995; 36(12): 2287-9.

[116] Macdonald LR, Patt BE, Iwanczyk JS, W. TBM, Wang Y, Frey EC, *et al*. Pinhole SPECT of mice using the LumaGEM gamma camera. IEEE Trans Nucl Sci 2001; 48: 830-836.

[117] McElroy DP, Macdonald LR, Beekman FJ, Wang Y, Patt BE, Iwanczyk JS, *et al*. Evaluation of A-SPECT: a desktop pinhole SPECT system for small animal imaging. Nucl Sci Symp Conf Rec 2002; 3: 1835-1839.

[118] Jeavons AP, Chandler RA, Dettmar CAR. A 3D HIDAC-PET camera with sub-millimetre resolution for imaging small animals. Nucl Sci Trans 1999; 46: 468-473.

[119] Tai C, Chatziioannou A, Siegel S, Young J, Newport D, Goble RN, *et al*. Performance evaluation of the microPET P4: a PET system dedicated to animal imaging. Phys Med Biol 2001; 46(7): 1845-62.

[120] Lewis JS, Achilefu S, Garbow JR, Laforest R, Welch MJ. Small animal imaging. current technology and perspectives for oncological imaging. Eur J Cancer 2002; 38(16): 2173.

[121] Eckelman WC, Reba RC, Gibson RE, Rzeszotarski WJ, Vieras F, Mazaitis JK, *et al*. Receptor-binding radiotracers: a class of potential radiopharmaceuticals. J Nucl Med 1979; 20(4): 350-7.

[122] Katzenellenbogen JA, Heiman DF, Carlson KE, editors. *In vitro* and *in vivo* steroid receptor assays in the design of estrogen radiopharmaceuticals. Boca Raton, FL: CRC Press 1982.

[123] Eckelman WC. Mechanism of target specific uptake using examples of muscarinic receptor binding radiotracers. In: Welch MJ, Redvanly C, editors. Radiochemistry and Applications. West Sussex: John Wiley and Sons 2002.

[124] Passchier J, Gee A, Willemsen A, Vaalburg W, van Waarde A. Measuring drug-related receptor occupancy with positron emission tomography. Methods 2002; 27(3): 278.

[125] Hume SP, Gunn RN, Jones T. Pharmacological constraints associated with positron emission tomographic scanning of small laboratory animals. Eur J Nucl Med 1998; 25(2): 173-6.

[126] Chow PL, Rannou FR, Chatziioannou A. Attenuation correction for a 3-D small animal PET tomograph, using x-ray microCT. In: Acad Mol Im; 2002; Los Angeles, CA 2002.

[127] Goertzen AL, Meadors K, Silverman RW, Cherry SR. Simultaneous PET and x-ray CT imaging of the mouse. In: Acad Mol Im; 2002; Los Angeles, CA 2002.

[128] Meltzer CC, Leal JP, Mayberg HS, Wagner HN Jr, Frost JJ. Correction of PET data for partial volume effects in human cerebral cortex by MR imaging. J Comput Assist Tomogr 1990; 14(4): 561-70.

[129] Rousset OG, Ma Y, Evans AC. Correction for partial volume effects in PET: principle and validation. J Nucl Med 1998; 39(5): 904-11.

[130] Da Silva AJ, Tang HR, Wong KH, Wu MC, Dae MW, Hasegawa BH. Absolute quantification of regional myocardial uptake of 99mTc-sestamibi with SPECT: experimental validation in a porcine model. J Nucl Med 2001; 42(5): 772-9.

[131] Aston JA, Cunningham VJ, Asselin MC, Hammers A, Evans AC, Gunn RN. Positron emission tomography partial volume correction: estimation and algorithms. J Cereb Blood Flow Metab 2002; 22(8): 1019-34.

[132] Cho K, Kumiata S, Okada S, Kumazaki T. Development of respiratory gated myocardial SPECT system. J Nucl Cardiol 1999; 6(1 Pt 1): 20-8.

[133] Nehmeh SA, Erdi YE, Ling CC, Rosenzweig KE, Schoder H, Larson SM, *et al*. Effect of respiratory gating on quantifying PET images of lung cancer. J Nucl Med 2002; 43(7): 876-81.

[134] Herrero P, Markham J, Myears DW, Weiheimer CJ, Bergmann SR. Measurement of myocardial blood flow with positron emission tomography: correction for count spillover and partial volume effects. Math Comput Model 1988; 11: 807-812.

[135] Iida H, Rhodes CG, de Silva R, Yamamoto Y, Araujo LI, Maseri A, *et al*. Myocardial tissue fraction--correction for partial volume effects and measure of tissue viability. J Nucl Med 1991; 32(11): 2169-75.

[136] Iida H, Law I, Pakkenberg B, Krarup-Hansen A, Eberl S, Holm S, *et al*. Quantitation of regional cerebral blood flow corrected for partial volume effect using O-15 water and PET: I. Theory, error analysis, and stereologic comparison. J Cereb Blood Flow Metab 2000; 20(8): 1237-51.

[137] Green LA, Gambhir SS, Srinivasan A, Banerjee PK, Hoh CK, Cherry SR, *et al*. Noninvasive methods for quantitating blood time-activity curves from mouse PET images obtained with fluorine-18-fluorodeoxyglucose. J Nucl Med 1998; 39(4): 729-34.

[138] Sharp T, Kim JY, Dence CS, Jones LA, Mercer NM, Engelbach JA, *et al*. Quantification of cardiovascular metabolism in mice. Mol Imaging and Biol 2002; 4(4): S41.

[139] Kim JY, Sharp T, Herrero P, Engelbach JA, Mercer NM, Jones LA, *et al*. Quantification of F-18 FDG myocardial glucose utilization in mice with microPET. Mol Imaging and Biol 2002; 4(4): S38.

[140] Lapointe D, Cadorette J, Rodrigue S, Rouleau D, Lecomte r. A microvolumetric blood counter/sampler for metabolic PET studies in small animals. IEEE Trans Nucl Sci 1998; 45: 2195-2199.

[141] Wu HM, Huang SC, Allada V, Wolfenden PJ, Schelbert HR, Phelps ME, *et al*. Derivation of input function from FDG-PET studies in small hearts. J Nucl Med 1996; 37(10): 1717-22.

[142] Lee JS, Lee DS, Ahn JY, Cheon GJ, Kim SK, yeo JS, *et al*. Blind separation of cardiac components and extraction of input function from $H_2{}^{15}O$ dynamic myocardial PET using independent component analysis. J Nucl Med 2001; 42: 938-43.

[143] Lee JS, Lee DD, Choi S, Park KS, Lee DS. Non-negative matrix factorization of dynamic images in nuclear medicine. Nucl Sci Symp Conf Rec 2001.

[144] Wu HM, Stout D, Shoghi-Jodid K, C. S, Chatziioannou A, Huang SC. Derivation of input function from dynamic FDG microPET images of mice. Mol Imaging and Biol 2002; 4(4): S43.

[145] Takikawa S, Dhawan V, Spetsieris P, Robeson W, Chaly T, Dahl R, *et al*. Noninvasive quantitative fluorodeoxyglucose PET studies with an estimated input function derived from a population-based arterial blood curve. Radiology 1993; 188(1): 131-6.

[146] Shiozaki T, Sadato N, Senda M, Ishii K, Tsuchida T, Yonekura Y, *et al*. Noninvasive estimation of FDG input function for quantification of cerebral metabolic rate of glucose: optimization and multicenter evaluation. J Nucl Med 2000; 41(10): 1612-8.

[147] Hume SP, Myers R, Bloomfield PM, Opacka-Juffry J, Cremer JE, Ahier RG, *et al*. Quantitation of carbon-11-labeled raclopride in rat striatum using positron emission tomography. Synapse 1992; 12(1): 47-54.

[148] Lammertsma AA, Hume SP. Simplified reference tissue model for PET receptor studies. Neuroimage 1996; 4(3 Pt 1): 153-8.

[149] Sun X, Annala AJ, Yaghoubi SS, Barrio JR, Nguyen KN, Toyokuni T, *et al*. Quantitative imaging of gene induction in living animals. Gene Ther 2001; 8(20): 1572-9.

[150] Yu Y, Annala AJ, Barrio JR, Toyokuni T, Satyamurthy N, Namavari M, *et al*. Quantification of target gene expression by imaging reporter gene expression in living animals. Nat Med 2000; 6(8): 933-7.

[151] Sharma V, Luker GD, Piwnica-Worms D. Molecular imaging of gene expression and protein function *in vivo* with PET and SPECT. J Magn Reson Imaging 2002; 16(4): 336-51.

[152] Gambhir SS, Herschman HR, Cherry SR, Barrio JR, Satyamurthy N, Toyokuni T, *et al*. Imaging transgene expression with radionuclide imaging technologies. Neoplasia 2000; 2(1-2): 118-38.

[153] Mayer-Kuckuk P, Banerjee D, Malhotra S, Doubrovin M, Iwamoto M, Akhurst T, *et al*. Cells exposed to antifolates show increased cellular levels of proteins fused to dihydrofolate reductase: a method to modulate gene expression. Proc Natl Acad Sci USA 2002; 99(6): 3400-5.

[154] Haubner R, Wester HJ, Weber WA, Mang C, Ziegler SI, Goodman SL, *et al*. Noninvasive imaging of alpha(v)beta3 integrin expression using 18F-labeled RGD-containing glycopeptide and positron emission tomography. Cancer Res 2001; 61(5): 1781-5.

[155] Thanos PK, Taintor NB, Alexoff D, Vaska P, Logan J, Grandy DK, *et al*. *In vivo* Comparative Imaging of Dopamine D2 Knockout and Wild-Type Mice with (11)C-Raclopride and MicroPET. J Nucl Med 2002; 43(11): 1570-1577.

[156] Moore TH, Osteen TL, Chatziioannou TF, Hovda DA, Cherry TR. Quantitative assessment of longitudinal metabolic changes *in vivo* after traumatic brain injury in the adult rat using FDG-microPET. J Cereb Blood Flow Metab 2000; 20(10): 1492-501.

[157] Kornblum HI, Araujo DM, Annala AJ, Tatsukawa KJ, Phelps ME, Cherry SR. *In vivo* imaging of neuronal activation and plasticity in the rat brain by high resolution positron emission tomography (microPET). Nat Biotechnol 2000; 18(6): 655-60.

[158] Kornblum HI, Cherry SR. The use of microPET for the development of neural repair therapeutics: studies in epilepsy and lesion models. J Clin Pharmacol 2001; Suppl: 55S-63S.

[159] Araujo DM, Cherry SR, Tatsukawa KJ, Toyokuni T, Kornblum HI. Deficits in striatal dopamine D(2) receptors and energy metabolism detected by *in vivo* microPET imaging in a rat model of Huntington's disease. Exp Neurol 2000; 166(2): 287-97.

[160] Wu JC, Inubushi M, Sundaresan G, Schelbert HR, Gambhir SS. Positron emission tomography imaging of cardiac reporter gene expression in living rats. Circulation 2002; 106(2): 180-3.

[161] Kudo T, Fukuchi K, Annala AJ, Chatziioannou AF, Allada V, Dahlbom M, *et al*. Noninvasive measurement of myocardial activity concentrations and perfusion defect sizes in rats with a new small-animal positron emission tomograph. Circulation 2002; 106(1): 118-23.

[162] Adonai N, Nguyen KN, Walsh J, Iyer M, Toyokuni T, Phelps ME, *et al*. *Ex vivo* cell labeling with 64Cu-pyruvaldehyde-bis(N4-methylthiosemicarbazone) for imaging cell trafficking in mice with positron-emission tomography. Proc Natl Acad Sci USA 2002; 99(5): 3030-5.

[163] Johnstrom P, Harris NG, Fryer TD, Barret O, Clark JC, Pickard JD, *et al*. (18)F-Endothelin-1, a positron emission tomography (PET) radioligand for the endothelin receptor system: radiosynthesis and *in vivo* imaging using microPET. Clin Sci (Lond) 2002; 103(Suppl 48): 4S-8S.

[164] Buckley RH. Gene therapy for SCID-a complication after remarkable progress. Lancet 2002; 360(9341): 1185-6.

[165] Tatum JL, Hoffman JM. Congressional update: report from the Biomedical Imaging Program of the National Cancer Institute. Imaging drug development. Acad Radiol 2000; 7(11): 1007-8.

[166] Chatziioannou AF, Cherry SR, Shao Y, Silverman RW, Meadors K, Farquhar TH, *et al*. Performance evaluation of microPET: a high-resolution lutetium oxyorthosilicate PET scanner for animal imaging. J Nucl Med 1999; 40(7): 1164-75.

[167] Walledge RJ, Manavaki R, Reader AJ, Jeavons AP, Julyan PJ, Zhao S, *et al*. Quad-HIDAC PET: comparison of four image reconstruction techniques for high resolution imaging. IEEE Nucl Sci Symp Conf Rec 2002: 1816-1820.

[168] Seidel J, Vaquero JJ, Green MV. Resolution uniformity and sensitivity of the NIH ATLAS small animal PET scanner: comparison to simulated LSO scanners without depth-of-interaction capability. IEEE Nucl Sci Symp Conf Rec 2001: 1555-1558.

[169] Green MV, Seidel J, Johnson CA, Vaquero JJ, Pascau J, Desco M. Towards high performance small animal positron emission tomography. Biomed Image Proc 2002: 369-372.

[170] Weber S, Bauer A, Herzog H, Kehren F, Muhlensiepen H, Vogelbruch J, *et al*. Recent results of the TierPET. IEEE Trans Nucl Sci 2000; 47: 1665-1669.

[171] Del Guerra A, Di Domenico g, Scandola M, Zavattini G. YAP-PET: first results of a small animal positron emission tomograph based on YAP crystals. IEEE Trans Nucl Sci 1998; 45: 3105-3108.

[172] Bruyndonckx P, Carnochan P, Younggang W, Duxbury D, Brooks R, White L, *et al*. The VUB-PET system: performance evaluation and applications for radiotracer validation and anticancer drug development. HiRes 1999: High Resolution Imaging in Small Animals; Amsterdam, Netherlands.

[173] Correia JA, Burnham CA, Kaufman D, Fischman AJ. Development of a small animal PET device with resolution approaching 1 mm. IEEE Nucl Sci Symp Conf Rec 1999; 46: 631-635.

[174] Rouze NC, Winkle W, Hutchins GD. IndyPET-a high resolution, high sensitivity dedicated research scanner. IEEE Nucl Sci Symp Conf Rec 1999; 3: 1460-1464.

[175] Lecomte R, Cadorette J, Rodrigue S, Bentoukia M, Rouleau D, Yao R, *et al*. A high resolution PET scanner based on avalanche photodiode detectors for animal studies. In: IEEE 17th Annual Conference 1995; p. 525-526.

[176] Ziegler SI, Pichler BJ, Boening G, Rafecas M, Pimpl W, Lorenz E, *et al*. A prototype high-resolution animal positron tomograph with avalanche photodiode arrays and LSO crystals. Eur J Nucl Med 2001; 28(2): 136-43.

[177] Zhang J, van Zijl PC, Mori S. Neuroimage 2002; 15: 892-901.

[178] Zhou J, Payen JF, Wilson DA, Traystman RJ, van Zijl PC. Using the amide proton signals of intracellular proteins and peptides to detect pH effects in MRI. Nat Med 2003; 9(8): 1085-90.

[179] Elsinga PH, Hendrikse NH, Bart J, Vaalburg W, van Waarde A. PET Studies on P-glycoprotein function in the blood-brain barrier: how it affects uptake and binding of drugs within the CNS. Curr Pharm Design 2004; 10(13): 1493-503.

[180] Kairemo KJ, Tahtinen M. Radiolabeled compounds in the development of cytotoxic agents. Curr Pharm Design 2004; 10(24): 2923-34.

[181] Perkins AC, Frier M. Radionuclide imaging in drug development. Curr Pharm Design 2004; 10(24): 2907-21.